



Helium Replacement in Italy

HeRe in Italy

Monte Carlo Simulations for neutron detectors

General approach and application to a specific case

Lina Quintieri

Frascati 2-3 December 2013

Outlook

- ◆ General remarks on MC methods for neutron transport and interaction with matter
- ◆ FLUKA, Geant4, MCNPX (PHYTS): a brief description and comparison
- ◆ Example of neutron detector design and optimisation by MC codes: the Gem-SideOn detector, developed in the frame of the research and development of innovative detectors to tackle the ^3He replacement,
- ◆ Benchmark test case: First preliminary comparison MC versus experimental results
- ◆ Conclusion & future plan

He-3 crisis and development of new efficient neutron detectors

Ref : Bruno Guerard (ILL) & Karl Zeitelhack (FRM II)

- ◆ ^3He is a by product of Tritium production for use in nuclear weapons by Tritium β -decay into ^3He with a half life of 12.3 years.
- ◆ Only the US and Russia are providing significant amounts of ^3He . With the end of the Cold War the ^3He production from Tritium decay has been reduced significantly and since September 2001 the demand of ^3He has increased drastically due to security program launched in US and other countries
 1. severe depletion of the existing ^3He stockpile and shortage
 2. Cost increase by a factor of 25, from 80 €/l up to 2000 €/l
- ◆ ^3He demand for neutron scattering in 2009 – 2015 is estimated to 125 kl and the projected demand for US security applications is 100 kl for a ≈ 20 kl/year available (US+Russia)

In this frame it is easy to understand the strong importance of MC simulations as a valuable and “costless” tool to address the research toward new neutron detector in alternative to the ^3He

MC methods: general remarks

- ◆ Deterministic methods provide more exact solutions of approximate models, whereas Monte Carlo methods provide approximate solutions of more exact models (stochastic events)
- ◆ MC method is eminently suited to study stochastic processes, particularly radiation transport, such as motion of photons and neutrons and charged particles through matter.
- ◆ Monte Carlo simulations play an important role in optimising detectors. The method uses probabilities and random sampling instead to give an accurate picture of what can happen. Statistically the random samplings will most often demonstrate the most likely possibilities
- ◆ Experimental verification would not only be difficult to accomplish but expensive as well. Monte Carlo allows us to simulate an actual physical experiment and look at what most likely will happen. This information helps us to optimize the detector without actually building it.

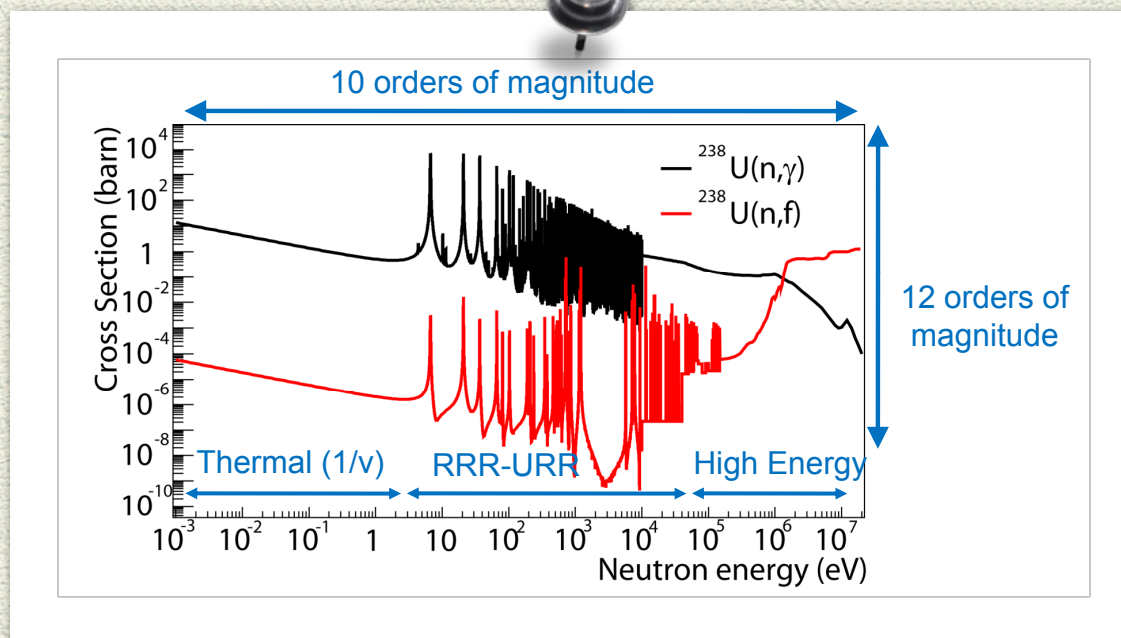
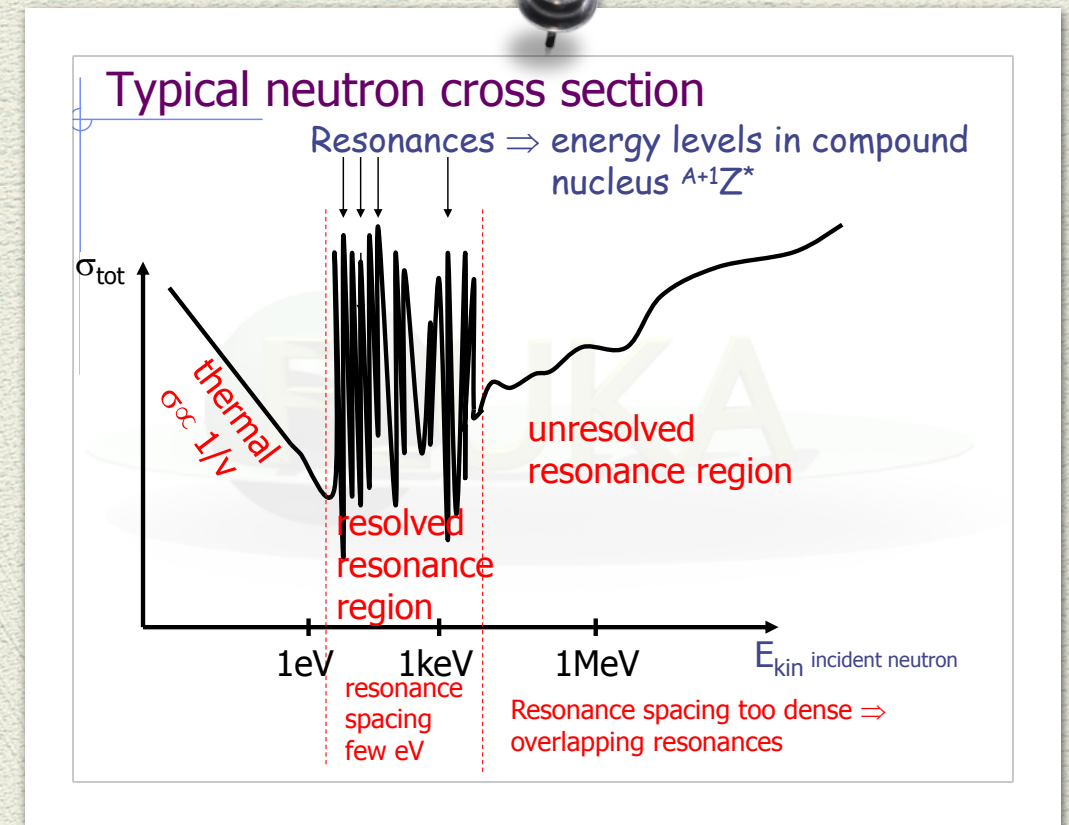
MC simulation of Neutron Detector

- ◆ Since neutrons are neutral, the only way to detect the presence of one is if it either collides with an atom or gets captured by an atom. These collisions and captures excite the particles and eventually give off photons or charged particles whose signal are directly registered
- ◆ It isn't the neutron itself but the photons or charged particles from the collisions which can be picked up and that which tell us that a neutron was even present. Efficiency is determined by: Efficiency = N_c/N , where N is the total number of neutrons that enter a cell and N_c is the number of neutrons that got captured (the importance in well tracking also secondary charged particles, as well).
- ◆ The possible types of interactions of a neutron with a nucleus include elastic scattering, inelastic scattering, absorption, and fission.
- ◆ Whether an interaction results in a neutron's being absorbed or scattered can be predicted only probabilistically (cross sections). Those probabilities, or cross sections, for the nuclei of the medium through which neutron passes are necessary input to solving the problem at hand.
- ◆ Also needed is the probability density function for the distance a neutron travels without undergoing an interaction with a nucleus (in other words, the probability density function for the lengths of the straight-line paths composing the neutron's trajectory)

Evaluated Nuclear Data Libraries Files

ENDF (USA), JEFF (Europe), JENDL(Japan), BROND (Russia), CENDL(China).....

- Neutron cross sections are isotope, energy and reaction channel dependent, and cannot be predicted by any nuclear model with the required accuracy all over the extended energy range
- Provide neutron cross sections typically for $E < 20\text{MeV}$ for all channels
- Are stored as continuum + resonance parameters



Data Libraries

- There can exist discrepancies among them
- Not all the distributions do release the same information and in the same way

- In addition to the cross sections also the secondary particles produced in a neutron reaction are tabulated: (n,gamma), (n,f) etc
- It is convenient that the end user could choose among various cross section files

What can be simulated of a detector ?

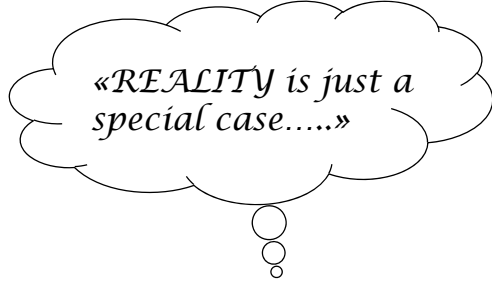
- ◆ Efficiency (depending upon major parameters: neutron energy, neutron incidence angle)
- ◆ Response Function and how it changes with major parameters
- ◆ Cross talk effect in complex geometries
- ◆ Performances study as a function of major parameters
- ◆ and much more
- ◆ but more intriguing **Separate un-separable effects**

Simulations can only give you back the physics that YOU HAVE PUT YOURSELF IN them.

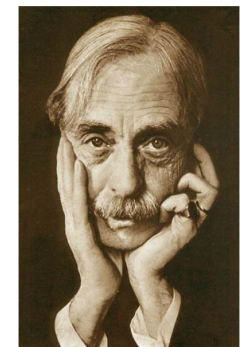
You will not discover «something new».

Separate un-separable effects

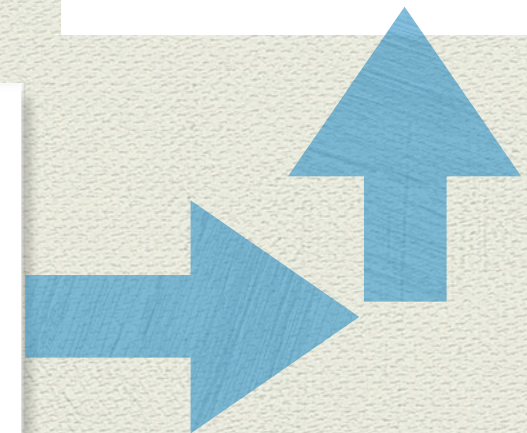
You can create unrealistic cases to help you better understanding your problem.



«*REALITY* is just a special case.....»



P. Valéry (1871 – 1945)



MC Errors and Limitations

MC simulations always have some errors which arise from the nature itself of the calculations. The Monte Carlo method involves calculating the average or probable behaviour of a system by observing the outcomes of a large number of trials (histories), after simulating the physical events responsible for the behaviour. These errors are

- ◆ statistical uncertainty (in analogue mode: $1/\sqrt{N}$).

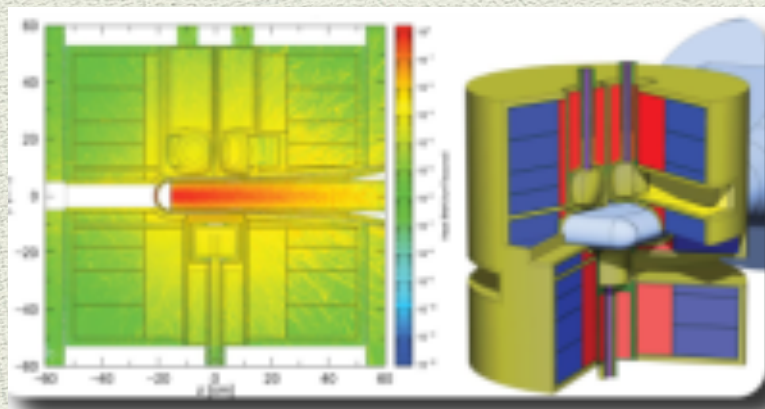
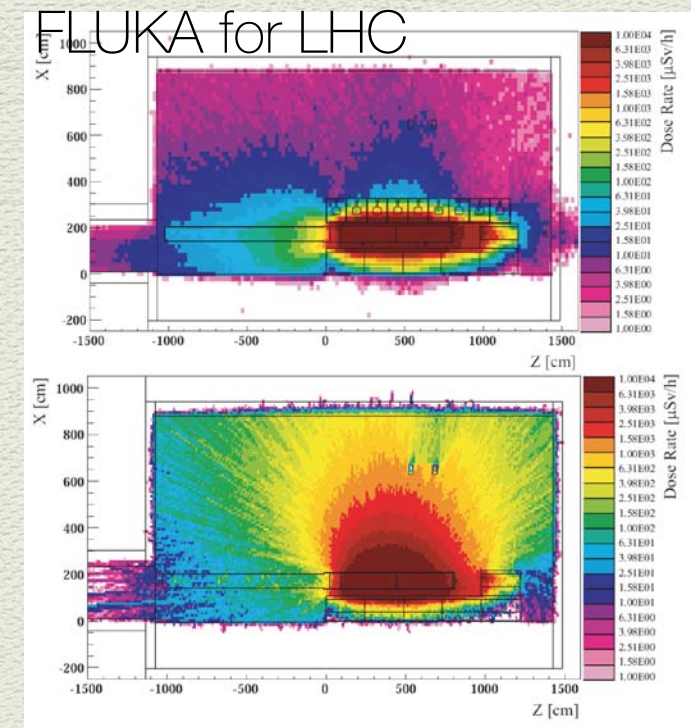
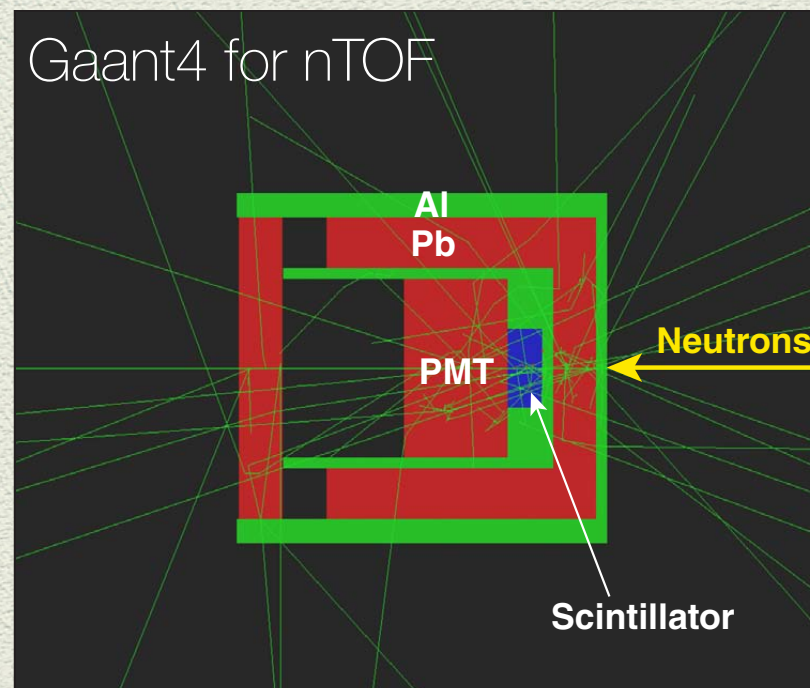
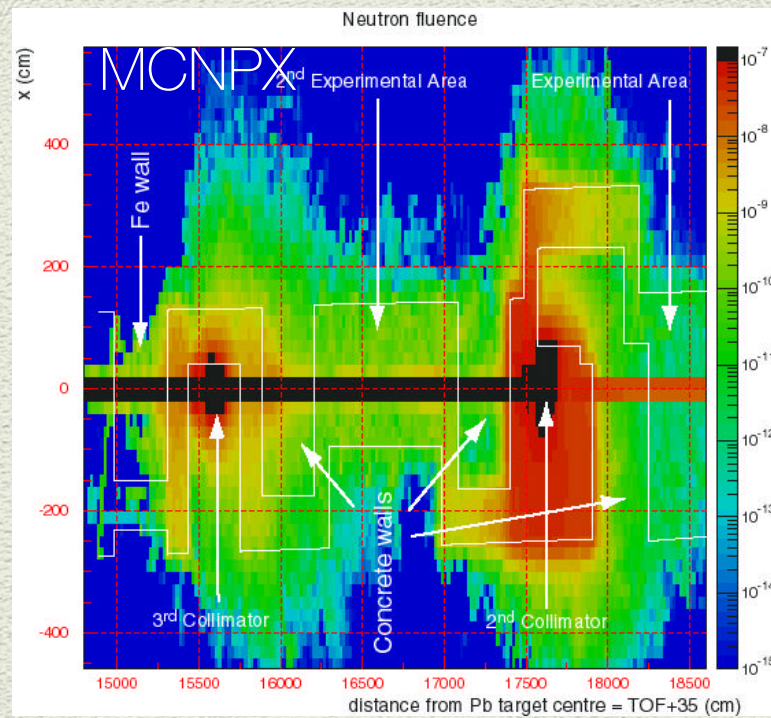
Moreover there are errors due to

- ◆ discrepancies in material composition and geometry
- ◆ errors in nuclear data libraries and theoretical models

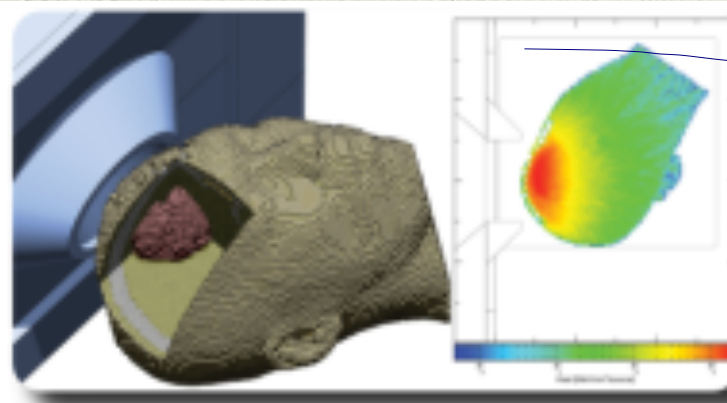
Often variance reduction techniques are required to improve the result accuracy (increasing statistics using weight for secondaries, in order to not affect the physics)

MC codes for tracking neutrons: Fluka, Geant4, MCNPX, PHits

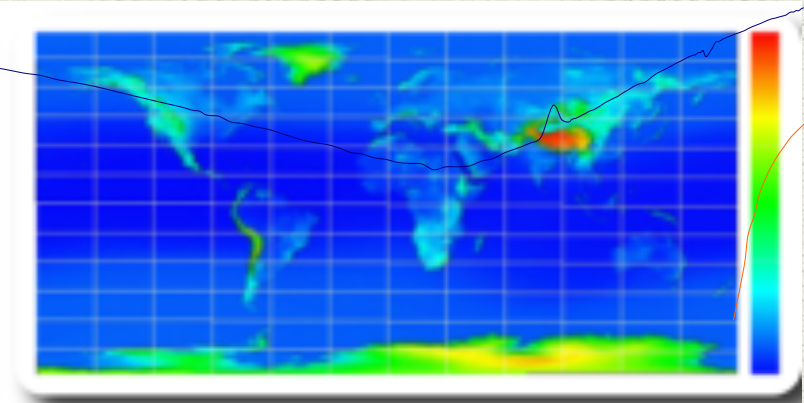
From reactor to space physics:



Accelerator



Radiotherapy



Space radiation

Fluka, Geant4, MCNP/x, PHits

- ◆ They are general-purpose Monte Carlo codes
- ◆ All these codes can reproduce geometric 3D configurations of materials and simulate particle transport through them.
- ◆ The extensive output includes all of this information, and allows calculating the efficiency of neutron capture inside the detector.
- ◆ These softwares enable us to accurately predict the effectiveness of different parameter variations on the detector performances
- ◆ Using probabilities from known cross sections and/or models, they can count: particle flux, particle collisions, particle captures and much more...
- ◆ The data are not built into modern Monte Carlo radiation transport codes but rather are available as separate data libraries. That stratagem permits the data libraries to be upgraded independently of the operational portion of the code

MC codes Comparison

(ref: G. McKinney et al. proc Science)

General	MCNPX	GEANT	FLUKA	PHITS
Version	MCNP6	Geant4.9	Fluka 2013	PHITS2.64
Lab. Affiliation	LANL	CERN,ESA,IN2P3PPARC,I NFN,LIP, KFK.SI.AC. TRIUMF	CERN INFN	JAEA, RIST KEK
Language	Fortran 90/C	C++	Fortran 77	Fortran 95/C
Cost	about 800 USD	Free	Free	Free
Release Format	Source & binary	Source & binary	Binary	Binary
Users	2000	~2000	~1000	120
Availability	RSICC	Open web	Open web after registration	Open web after registration
User Manual	470 pages	280 pages	387 pages	150 pages
Web Site	mcnpx.lanl.gov	cern.ch/geant4	www.fluka.org	phits.jaea.go.jp
Workshops	~7/year	~4/year	~1/year	-
Input Cards	~120	N/A	~85	100
Parallel Execution	Yes	Yes	Yes	Yes

Physics Capabilities

(ref: G. McKinney et al. proc Science)

Physics	MCNPX	GEANT	FLUKA	PHITS
Particles	34	68	68	38
Neutron Low High	Cont. (ENDF) Models	Cont. (ENDF) Models	Multigroup(260) Models	Cont. (ENDF) Modells
Proton Low High	Cont. (ENDF) Models	Models Models	Models Models	Models Models
Leptons Electron	ITS 3.0	Models/EEDL, EADL	Custom	ITS 3.0
Muon Neutrino Other	CSDA/decay Production Decay	Models Production Decay	Models Models Decay	CSDA/decay Models Models
Photons Optical x-ray/g Photonuclear	No ITS 3.0 Libraries (IAEA) CEM	Yes Models or EPDL97, EADL CHIPS	Yes Custom+EPDL97 PEANUT VMDM	No Custom Custom CEM
Fields (E/B)	2.6.D	Yes	Yes	Yes

A quick look inside the
codes

FLUKA

In FLUKA neutrons below 20 MeV are defined as low energy neutrons

Neutron interactions at higher energy are handled by FLUKA nuclear models

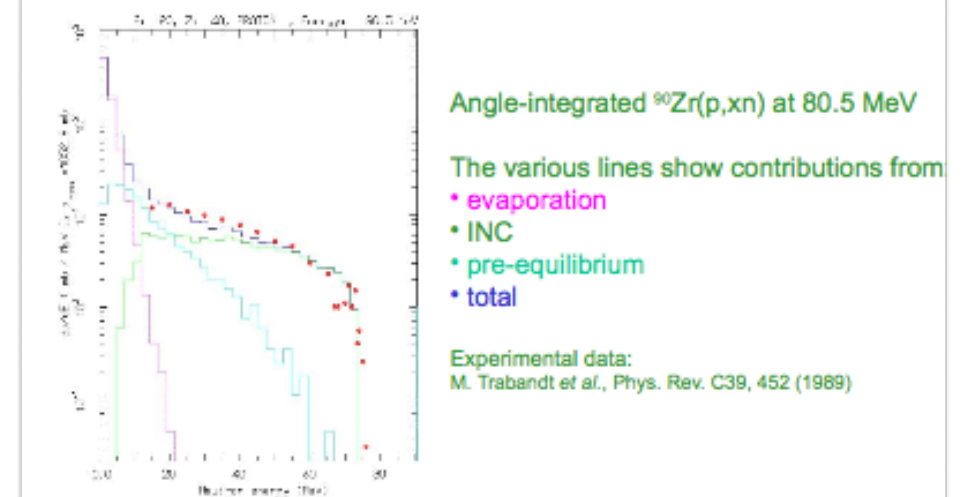
Transport and interactions of neutrons with energies below 20 MeV are handled by a dedicated library (Number of groups: 260 of approximately equal logarithmic width, whose 31 thermal)

Why are low Energy Neutrons special?

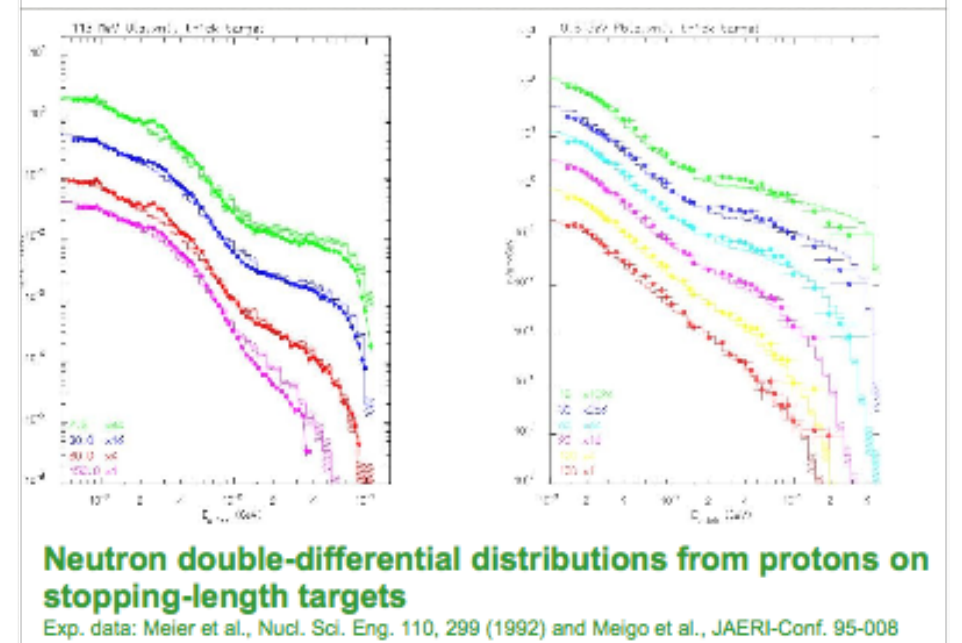
- neutron has no charge so it can interact with nuclei at low energies, e.g. meV (thermal)
- neutron cross sections are complicated
- cannot be calculated by models so that it is preferred to rely on data files

An example of validation

Physics: thin target example



Physics: thick target example



The default FLUKA neutron cross section library (originally prepared by G. Panini of ENEA) contains more than **250 different materials (natural elements or single nuclides)**, selected for their interest in physics, dosimetry and accelerator engineering. This library has a larger number of groups and a better resolution in the thermal energy range in respect to the original one

GEANT4

Below 20 MeV incident energy, Geant4 provides several models for treating neutron interactions in detail

The high precision neutron models (NeutronHP) are data-driven and depend on a large database of cross sections:

- the G4NDL database is available for download from the Geant4 web site
- elastic, inelastic, capture and fission models all use this isotope-dependent data

There are also models to handle thermal scattering from chemically bound atoms:

- G4HPThermalScatteringData,
- G4HPThermalScattering

(At thermal neutron energies, atomic motion, vibration and rotation of bound atoms affect the neutron scattering cross section, as well as the angular distribution of secondary neutrons .

The energy loss (or gain) of such scattered neutrons may be different from those from interactions with unbound atoms)

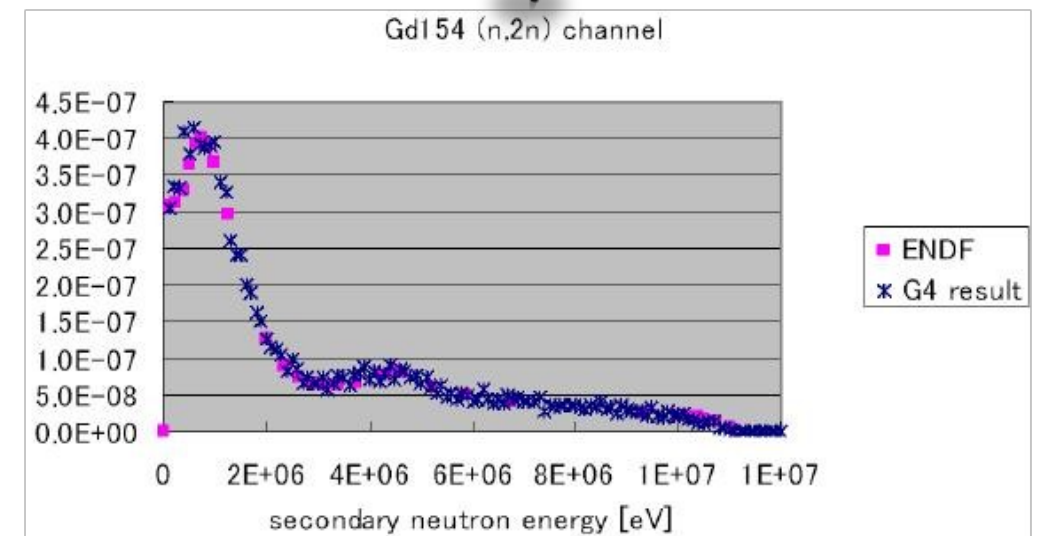
Geant4 Neutron Data Library (G4NDL)

Contains the data files for the high precision neutron models: includes both cross sections and final states:

Data are derived from the following evaluated data libraries: ENDF/B_VII.0, JEFF-3.1, JENDL-4.0,

The format of G4NDL is similar but not identical to that of ENDF evaluated libraries: difficult job to combine data from all the above libraries into one format

An example of validation



MCNPX

- 34 particle types (n,p,e,5 Leptons,11 Baryons,11 Mesons, 4 Light Ions)
- Continuous energy (roughly 0-0.1 TeV)
- Data libraries below ~ 150 MeV (n,p,e,h) and models otherwise

Pointwise cross-section data typically are used, although group-wise data also are available.

For neutrons, all reactions given in a particular cross-section evaluation (such as ENDF/B-VI) are accounted for.

Thermal neutrons are described by both the free gas and $S(\alpha,\beta)$ models.

The default continuous energy neutron transport data with 389 isotopes and 3 elements are from the ENDF70 library (based upon the ENDF/B-VII.0 evaluations).

LA--12212
DE92 004710

MCNP: Neutron Benchmark Problems

*Daniel J. Whalen
David A. Cardon
Jennifer L. Uhle
John S. Hendricks*

MASTER

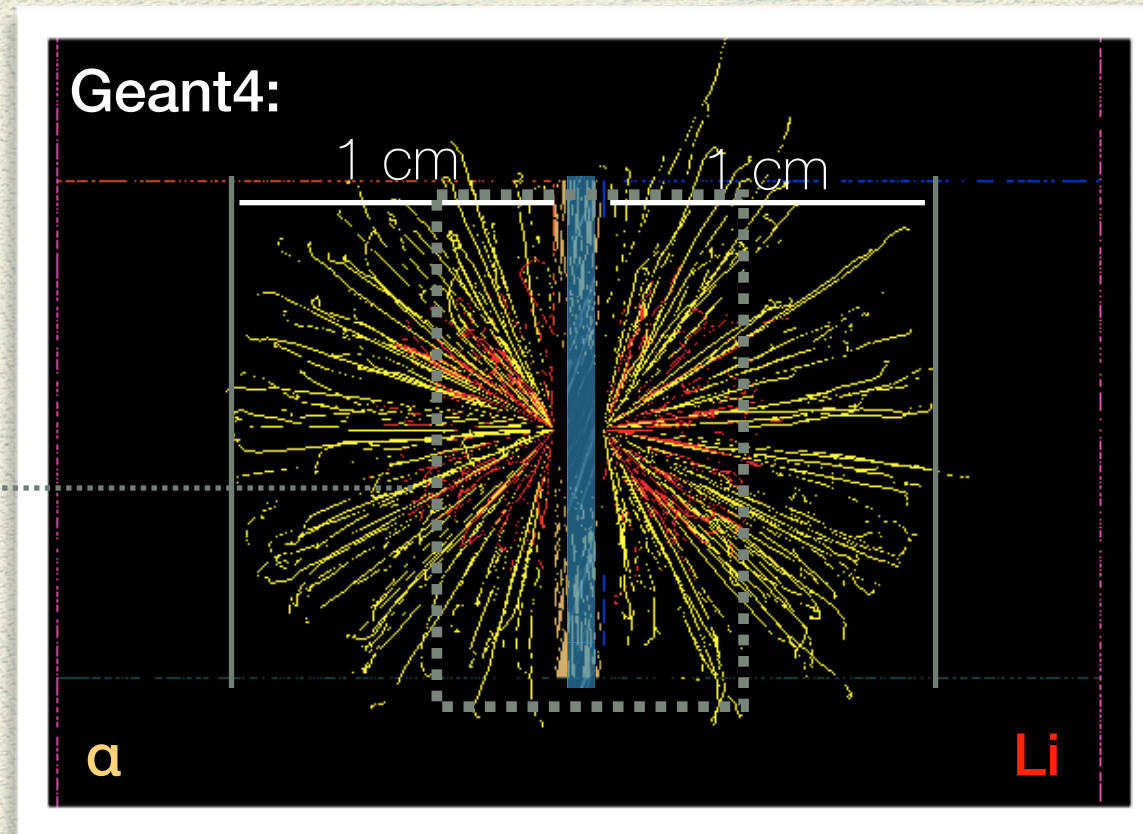
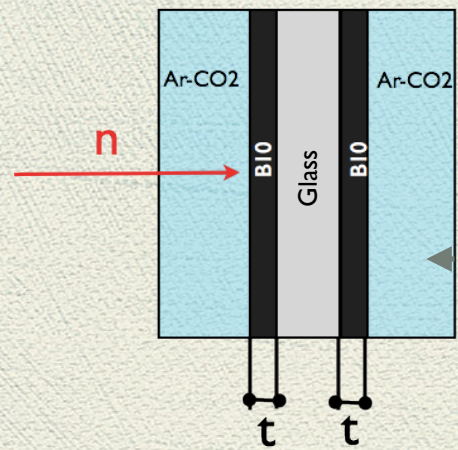
Los Alamos National Laboratory
Los Alamos, New Mexico 87545

**neutron shielding
experiments**

**neutron multiplication
experiments**

**neutron transport
experiments**

“MC optimisation of Gem SideOn Detector Design”



Results of simulations by Geant4 shown in figure refer to a primary neutron beam, perpendicular to the wider sheet surface, zero divergence, uniform in energy (25 meV kinetic energy without any energy spread),

Please Refer to the G.Claps talk for other details of this work

“MC optimisation of Gem SideOn Detector Design”

Nuclear Instruments and Methods in Physics Research A 729 (2013) 117–126



Contents lists available at [SciVerse ScienceDirect](#)

Nuclear Instruments and Methods in
Physics Research A

journal homepage: www.elsevier.com/locate/nima



A new ^3He -free thermal neutrons detector concept based
on the GEM technology



A. Pietropaolo ^{a,*}, F. Murtas ^b, G. Claps ^b, L. Quintieri ^{b,1}, D. Raspino ^c, G. Celentano ^d,
A. Vannozi ^d, O. Frasciello ^b

^a Consiglio Nazionale delle Ricerche, Istituto di Fisica del Plasma “P. Caldirola”, Milano, Italy

^b Istituto Nazionale di Fisica Nucleare, Laboratori Nazionali di Frascati, Frascati, Italy

^c Science and technology Facility Council, ISIS Facility, Chilton, Didcot, United Kingdom

^d ENEA Centro Ricerche Frascati, Frascati, Italy

ARTICLE INFO

Article history:

Received 20 November 2012

Received in revised form

29 May 2013

Accepted 12 June 2013

Available online 5 July 2013

Keywords:

GEM detector

Thermal neutrons detectors

Neutron instrumentation

ABSTRACT

A thermal neutron detector based on the Gas Electron Multiplier technology is presented. It is configured to let a neutron beam interact with a series of borated glass layers placed in sequence along the neutron path inside the device. The detector has been tested on beam both at the ISIS (UK) spallation neutron source and at the TRIGA reactor of ENEA, at the Casaccia Research Center, near Rome in Italy. For a complete characterization and description of the physical mechanism underlying the detector operation, several Monte Carlo simulations were performed using both Fluka and Geant4 code. These simulations are intended to help in seeking the optimal geometrical set-up and material thickness (converter layer, gas gap, sheet substrate) to improve the final detector design in terms of achieving the best detector efficiency possible.

© 2013 Elsevier B.V. All rights reserved.

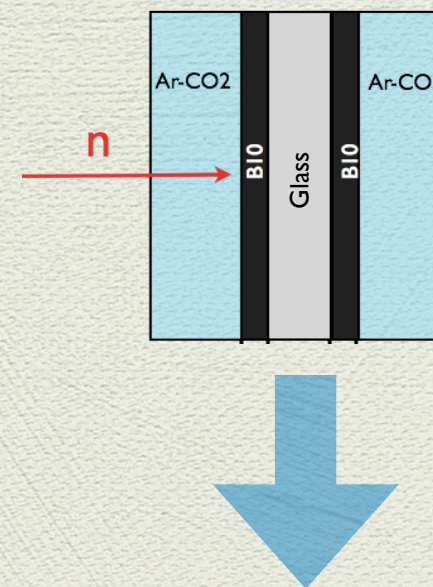
Results of simulations by Geant4 shown in figure refer to a primary neutron beam,
perpendicular to the wider sheet surface, zero divergence, uniform in energy (25 meV
kinetic energy without any energy spread),

Please Refer to the G.Claps talk for other details of this work

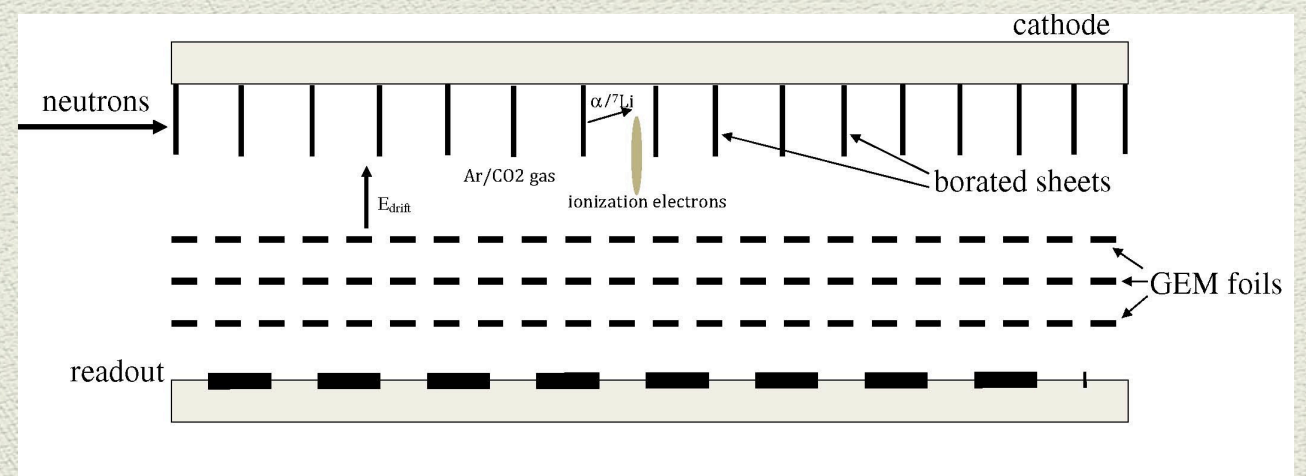
From single sheet validation to efficiency prediction for the complete detector

- ◆ We took a simple geometry to push the physics: a single sheet with thin two-side converter layer.
- ◆ We defined the conversion efficiency: charged particle that enter into the gas per unit absorbed neutron
- ◆ In this case the theoretic conversion efficiency and secondary particle distribution could be easily estimated (all the charged particles enter into the gas)
- ◆ As the B-10 thickness increases, the number of charged particles produced differs from the number of charged particles that reach the gas region and this effect becomes appreciable for B-10 thickness much lower than the alpha and ${}^7\text{Li}$ range values :the range of 1.47 MeV alphas and 0.84 MeV ${}^7\text{Li}$ ions in 10B is respectively about 3.6 μm and 2 μm).

Starting point: validation of the single sheet (300nm B-10)

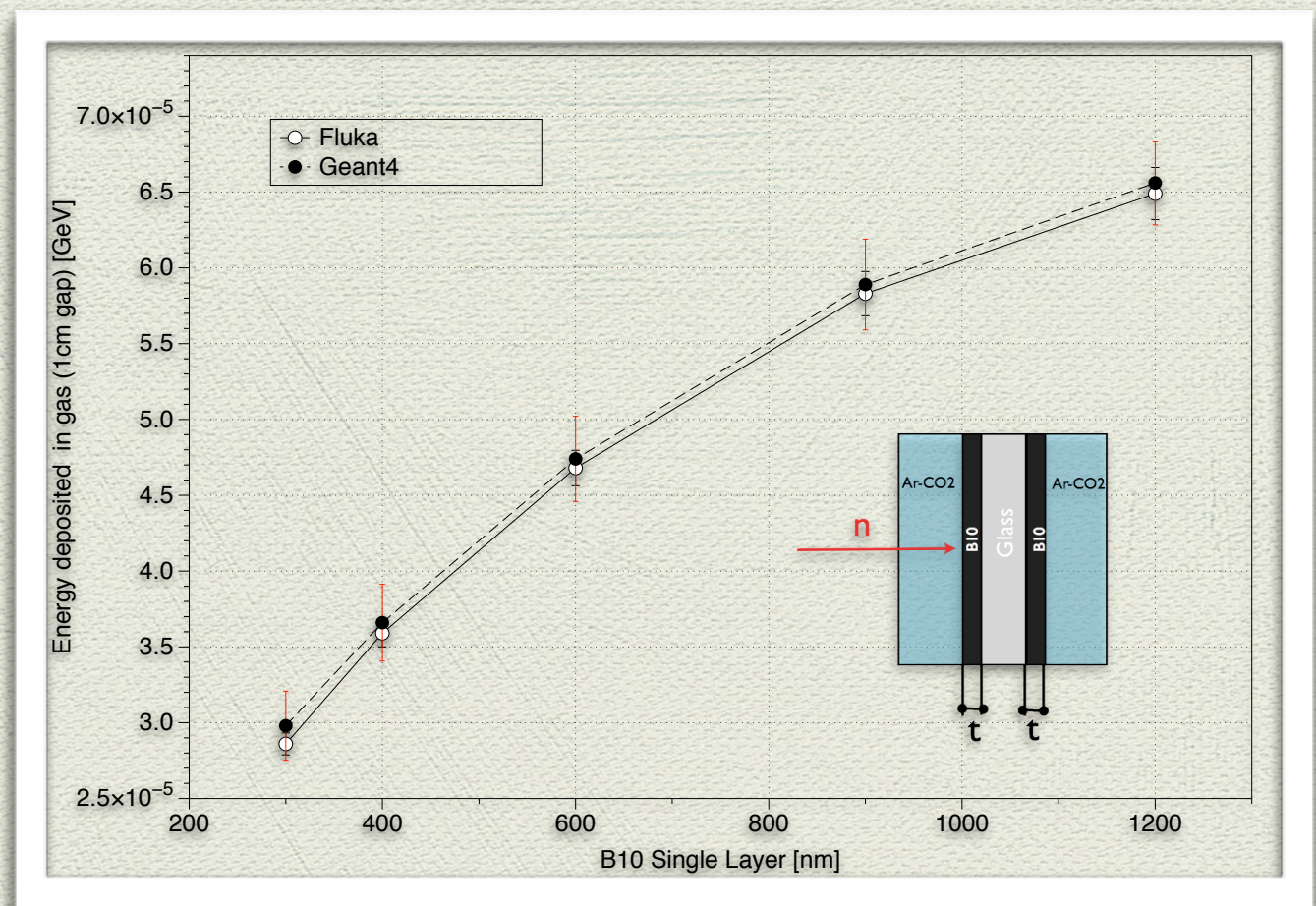
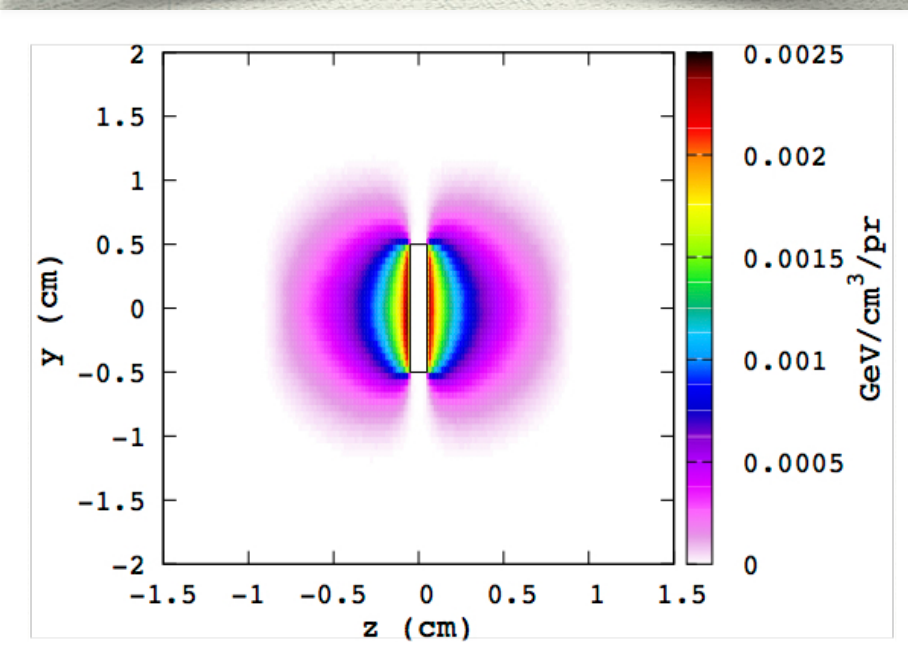
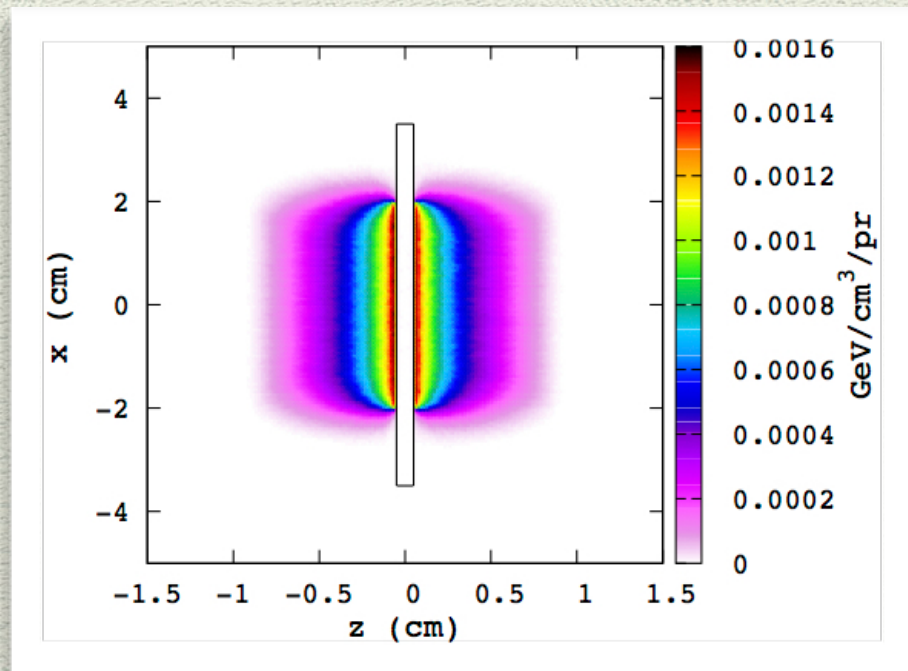


goal: to optimize the multiple sheet final design



Spatial energy deposition and particles fluence: detailed results for a 300 nm B-coated single sheet

FLUKA: Energy density deposition by alpha particles (simulated case: incident wide (4cmx1cm) neutron beam)



- Predicted energy deposition by the charged particles in the gas, for different converter thickness values (from 300 up to 1200 nm).
- Good agreement between the Geant4 and Fluka predictions.
- To highlight: increasing the B-10 thickness by a factor of 4 (from 300 nm to 1200 nm) the energy deposited in the gas increase only by a factor of 2.

Energy deposition and angular distribution in the gas around the single sheet

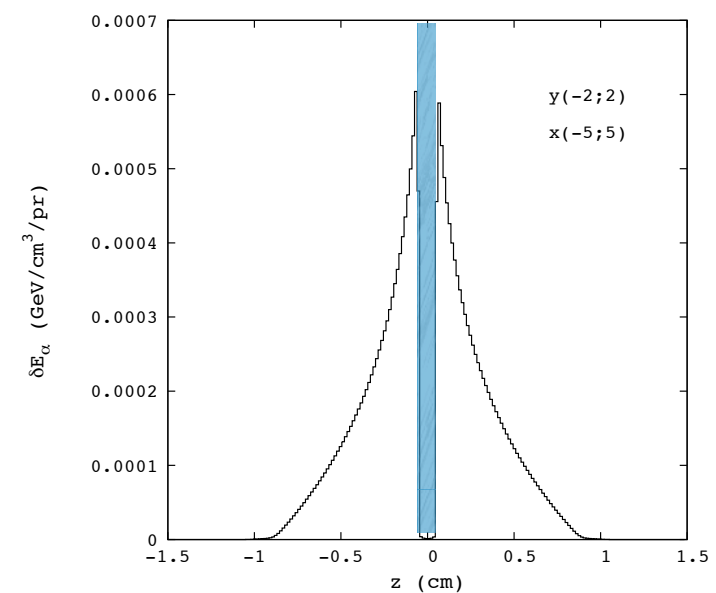
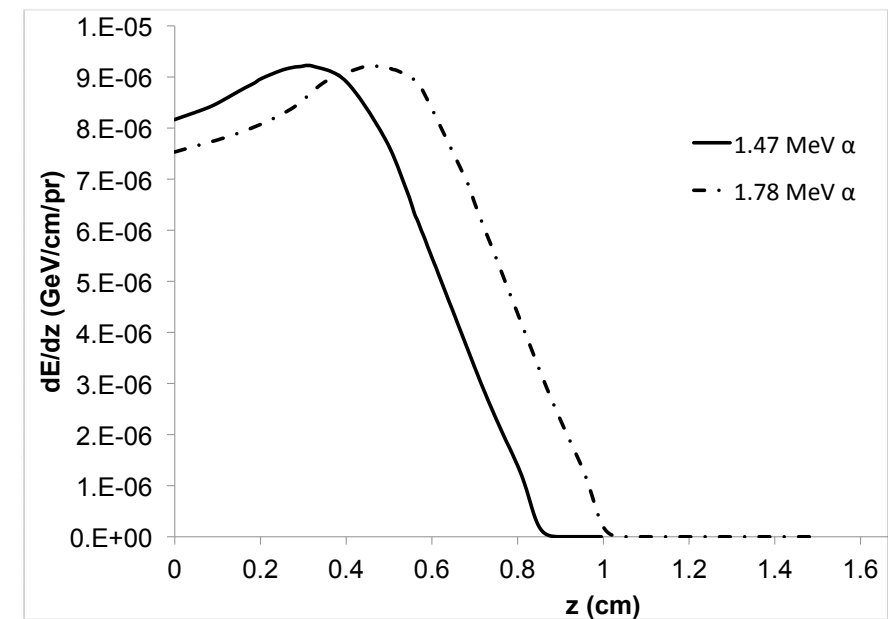
Ar/CO₂ mixture (70%/30%) at 1 atm: the linear energy deposition features as a broadened Bragg peak whose maximum for 1.47 MeV alpha is around 3 mm (5 mm for 1.78 alpha) and extends up to about 9 mm (11 mm for 1.78 MeV) (in accordance with SRIM code, too).

In spite of being mono-directional and mono-energetic, the alphas and ⁷Li that emerge from the ¹⁰B layers and enter the gas have angular isotropic distribution

Moreover particles entering into the gas have a continuous energy spectrum:

All these aspects are well taken into account in MC simulations and in particular in the efficiency estimation

The overall energy density profile (energy deposition from alphas and ⁷Li ions, respectively) in the simulated region (solid sheet and gas around) is obtained by cumulating the contributions of all the particles



Energy deposition and angular distribution in the gas around the single sheet

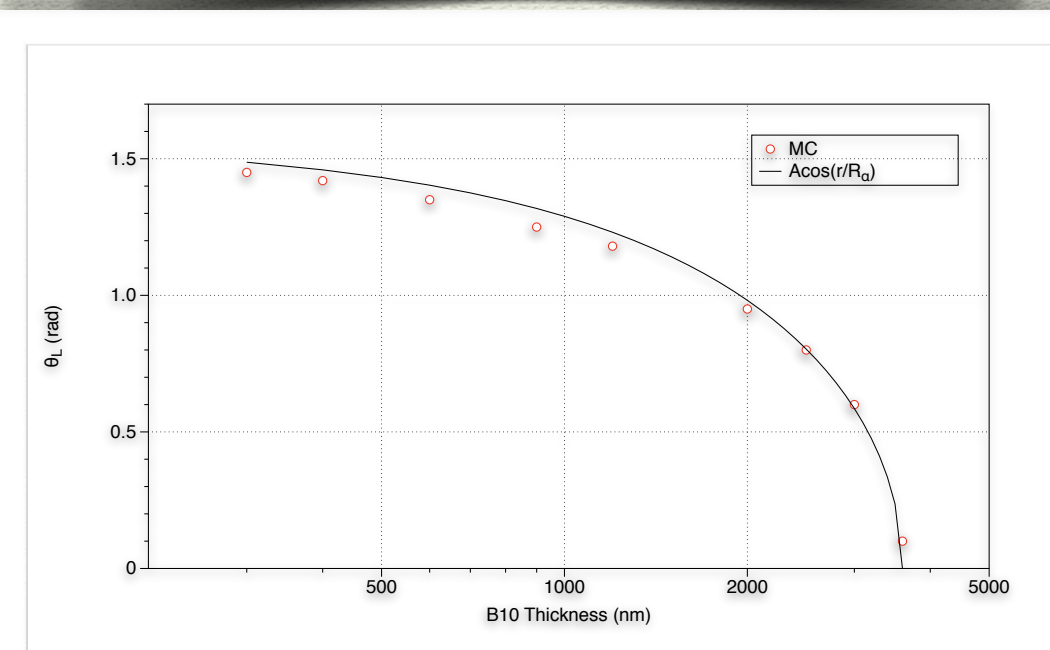
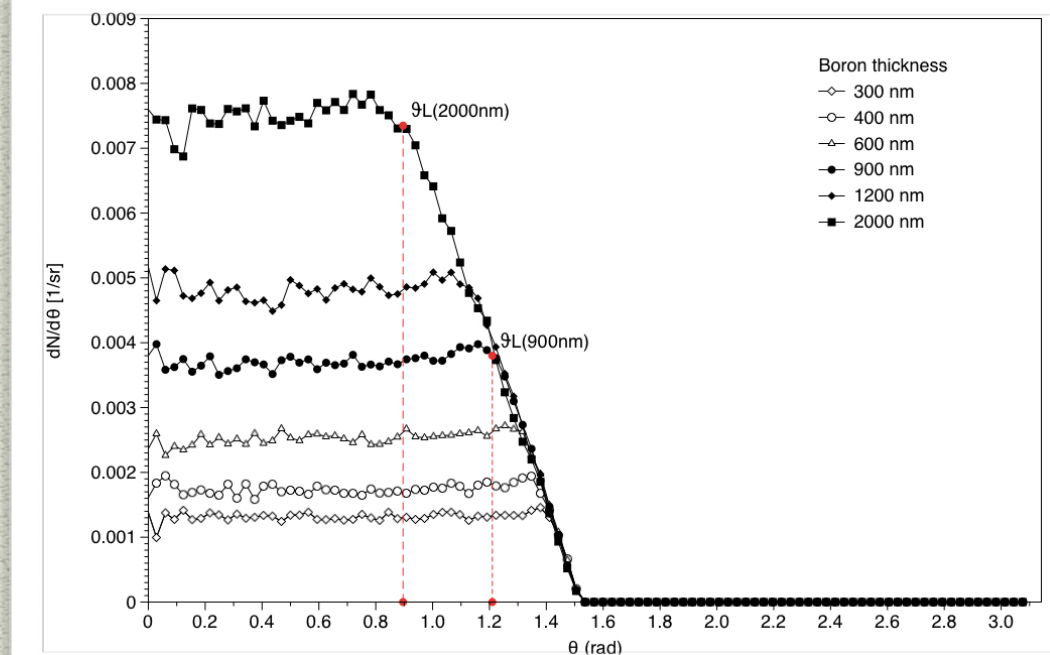
Ar/CO₂ mixture (70%/30%) at 1 atm: the linear energy deposition features as a broadened Bragg peak whose maximum for 1.47 MeV alpha is around 3 mm (5 mm for 1.78 alpha) and extends up to about 9 mm (11 mm for 1.78 MeV) (in accordance with SRIM code, too).

In spite of being mono-directional and mono-energetic, the alphas and ⁷Li that emerge from the ¹⁰B layers and enter the gas have angular isotropic distribution

Moreover particles entering into the gas have a continuous energy spectrum:

All these aspects are well taken into account in MC simulations and in particular in the efficiency estimation

The overall energy density profile (energy deposition from alphas and ⁷Li ions, respectively) in the simulated region (solid sheet and gas around) is obtained by cumulating the contributions of all the particles



Energy deposition and angular distribution in the gas around the single sheet

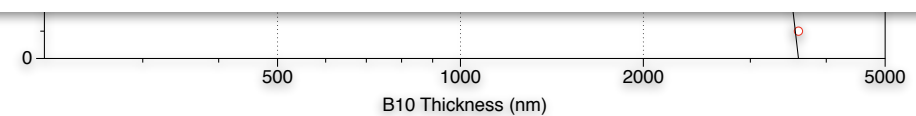
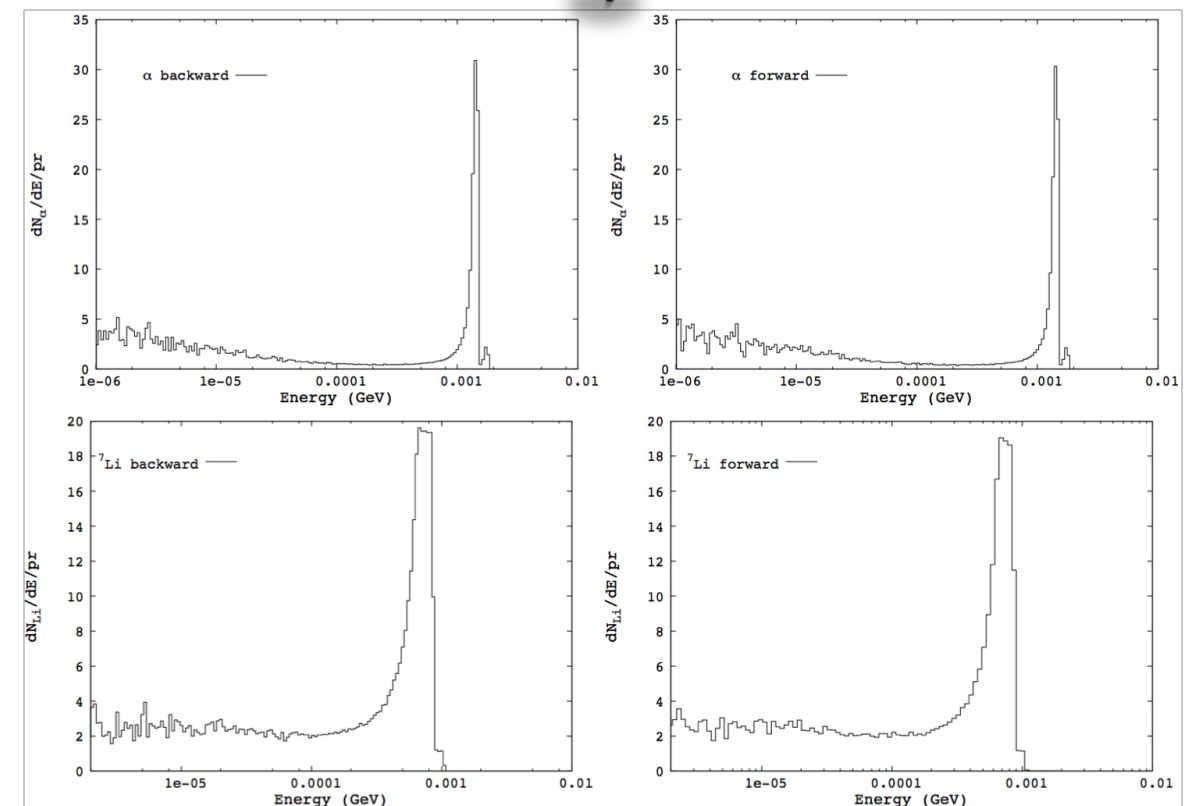
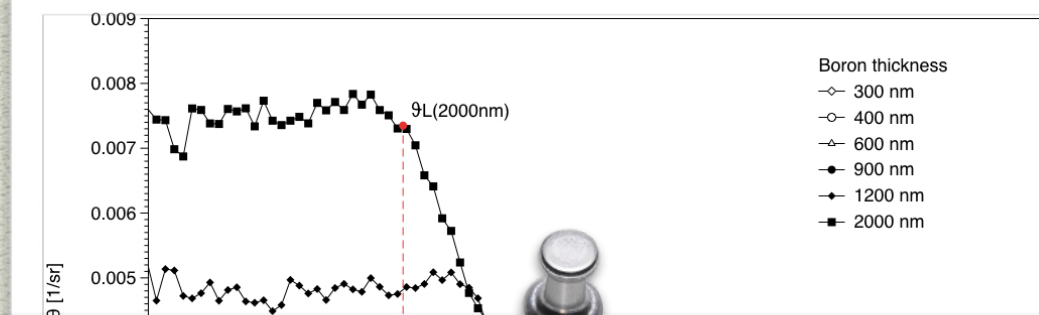
Ar/CO₂ mixture (70%/30%) at 1 atm: the linear energy deposition features as a broadened Bragg peak whose maximum for 1.47 MeV alpha is around 3 mm (5 mm for 1.78 alpha) and extends up to about 9 mm (11 mm for 1.78 MeV) (in accordance with SRIM code, too).

In spite of being mono-directional and mono-energetic, the alphas and ⁷Li that emerge from the ¹⁰B layers and enter the gas have angular isotropic distribution

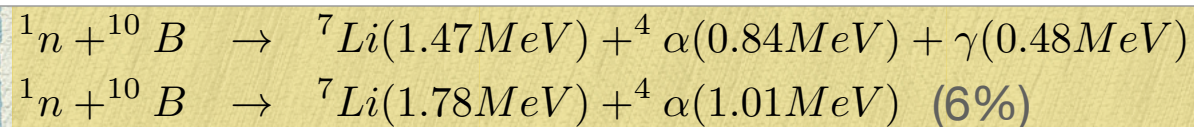
Moreover particles entering into the gas have a continuous energy spectrum:

All these aspects are well taken into account in MC simulations and in particular in the efficiency estimation

The overall energy density profile (energy deposition from alphas and ⁷Li ions, respectively) in the simulated region (solid sheet and gas around) is obtained by cumulating the contributions of all the particles



Conversion efficiency of a single two-side coated sheet as a function of the converter thickness (for thermal neutron)



$$RR \text{ [#reactions/cm}^3\text{/s]} = \Sigma \cdot \Phi \quad \text{where } \Sigma = N\sigma.$$

$$\epsilon = N\sigma \cdot (1 + P_1) \cdot \delta$$

P_1 is the fraction of neutrons surviving at depth x (those that do not interact up to x depth).

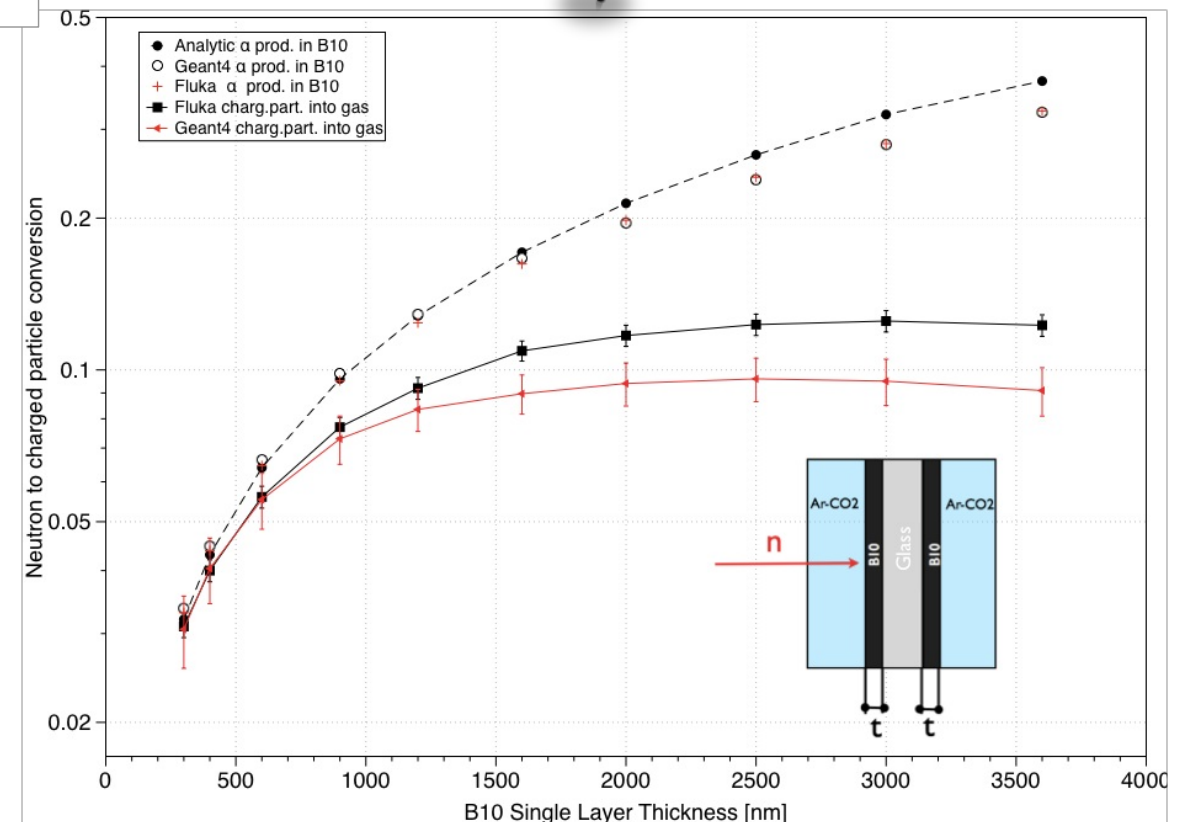
$$P_1 = \frac{I_x}{I_0} = e^{-\Sigma_{tot}x}$$

Table 1: B10 layer conversion efficiency as a function of thickness

B10-Thickness [nm]	Theoretical %	FLUKA %	Geant4 %	MCNPX %
300	3.2	3.3	3.37	in prog
400	4.3	4.38	4.47	-
600	6.4	6.46	6.63	-
900	9.6	9.52	9.84	-

As the ${}^{10}B$ thickness increases, the number of charged particles produced differs from the number of charged particles that reach the gas region. This effect becomes appreciable for ${}^{10}B$ thickness much thinner than the alpha and 7Li range values

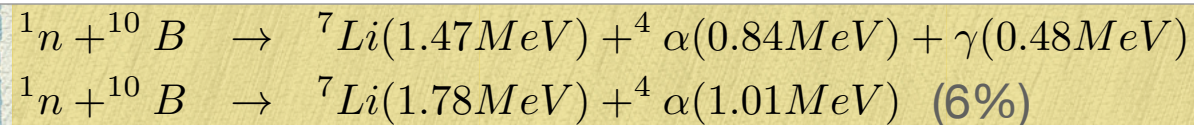
This is explained considering that the reaction products are emitted quite isotropically, so that the charged particles that are traveling in a solid angle larger than a certain angle have a higher probability to be absorbed inside the solid converter.



Estimated values of alphas produced per incident neutron inside the converter layers compared to charged particles (alphas and 7Li ions) leaving the ${}^{10}B$ layers and entering into the gas region (FLUKA, GEANT, anal.)

Analytic estimation: conservative approach, the dependence of the probability of neutron interaction upon the depth of converter layer has been neglected. This assumption could work well only for thin converter thickness.

Conversion efficiency of a single two-side coated sheet as a function of the converter thickness (for thermal neutron)



$$RR \text{ [#reactions/cm}^3\text{/s]} = \Sigma \cdot \Phi \quad \text{where } \Sigma = N\sigma.$$

$$\epsilon = N\sigma \cdot (1 + P_1) \cdot \delta$$

P_1 is the fraction of neutrons surviving at depth x (those that do not interact up to x depth).

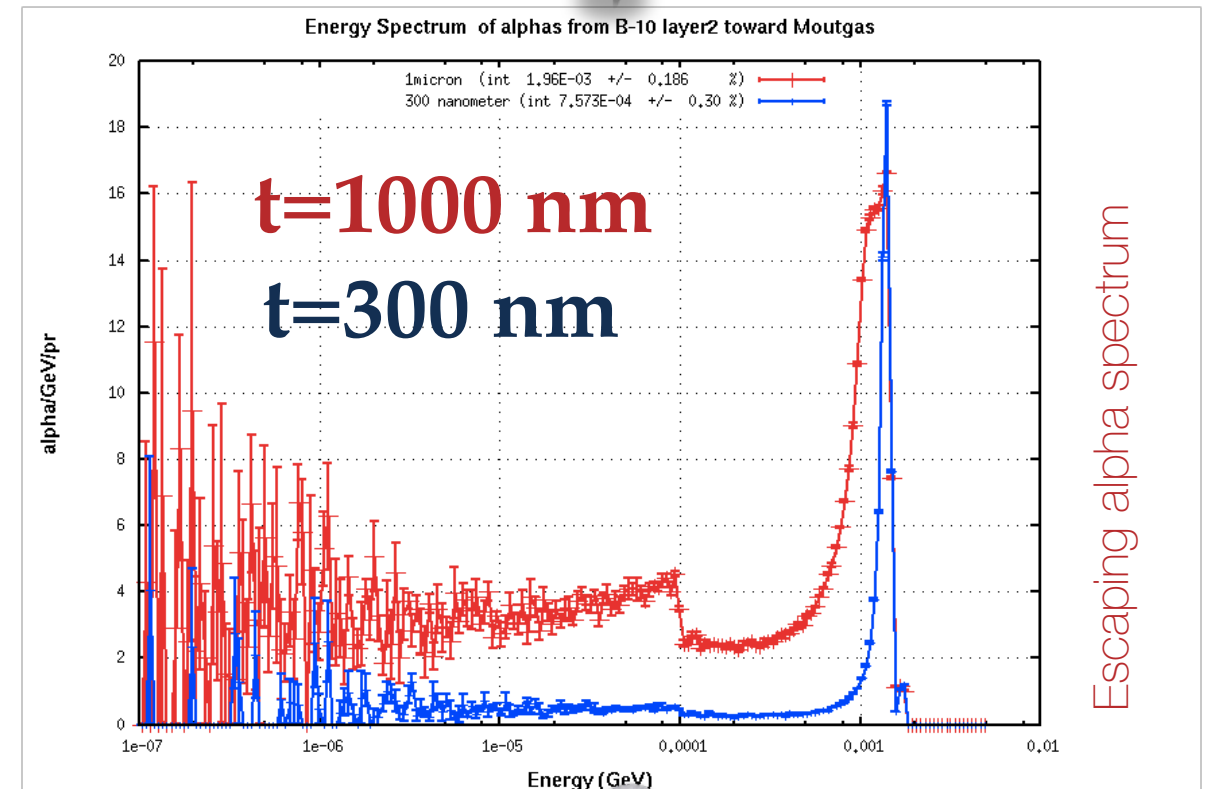
$$P_1 = \frac{I_x}{I_0} = e^{-\Sigma_{tot}x}$$

Table 1: B10 layer conversion efficiency as a function of thickness

B10-Thickness [nm]	Theoretical %	FLUKA %	Geant4 %	MCNPX %
300	3.2	3.3	3.37	in prog
400	4.3	4.38	4.47	-
600	6.4	6.46	6.63	-
900	9.6	9.52	9.84	-

As the ${}^{10}B$ thickness increases, the number of charged particles produced differs from the number of charged particles that reach the gas region. This effect becomes appreciable for ${}^{10}B$ thickness much thinner than the alpha and 7Li range values

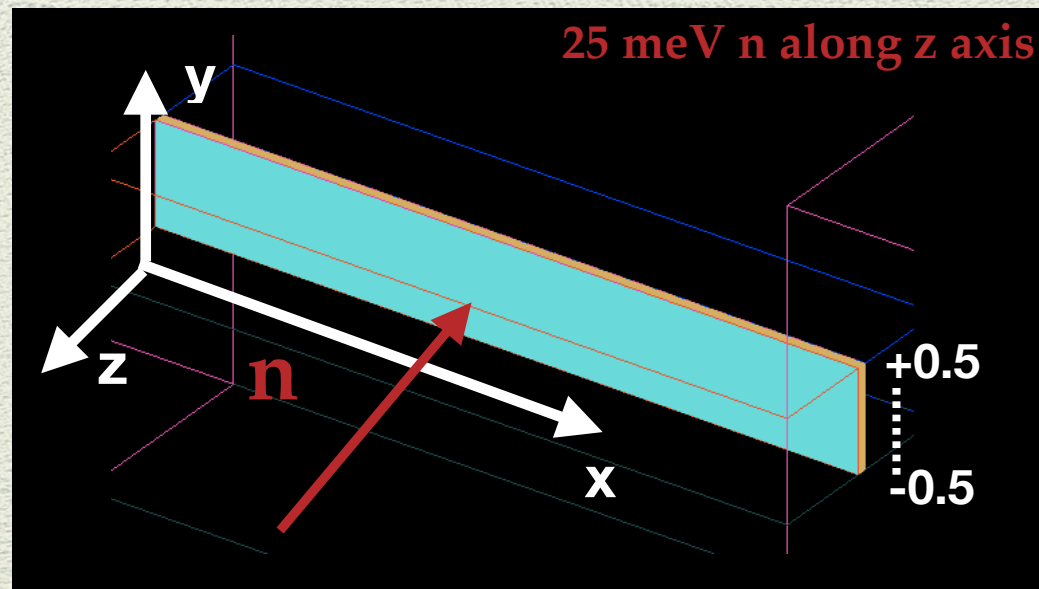
This is explained considering that the reaction products are emitted quite isotropically, so that the charged particles that are traveling in a solid angle larger than a certain angle have a higher probability to be absorbed inside the solid converter.



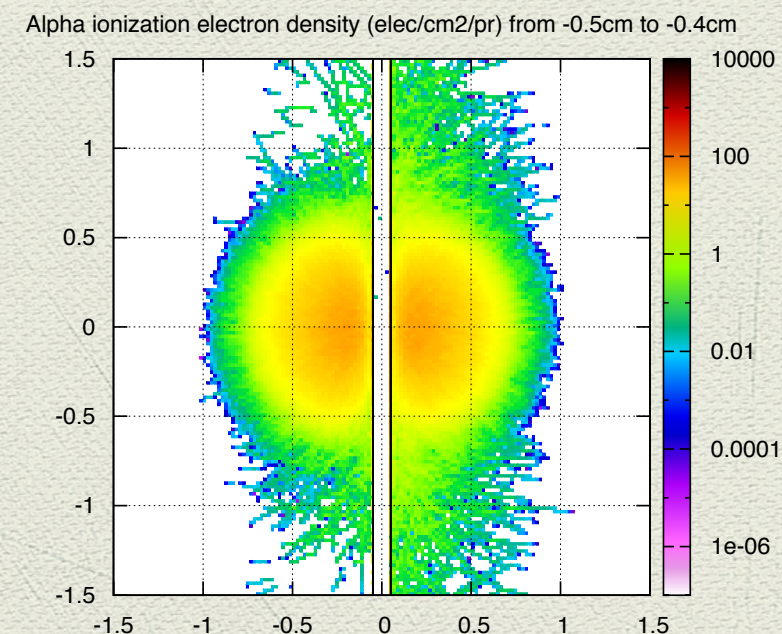
The continuous tail at lower energy and the broadened peaks in the spectra are due to the energy straggling that particles experience in passing through different thickness of boron before reaching the gas region: indeed, particles emitted at large angles travel over longer tracks inside the ${}^{10}B$ layer, thus losing much more

Indirectly derived electron density (transversal xz section)

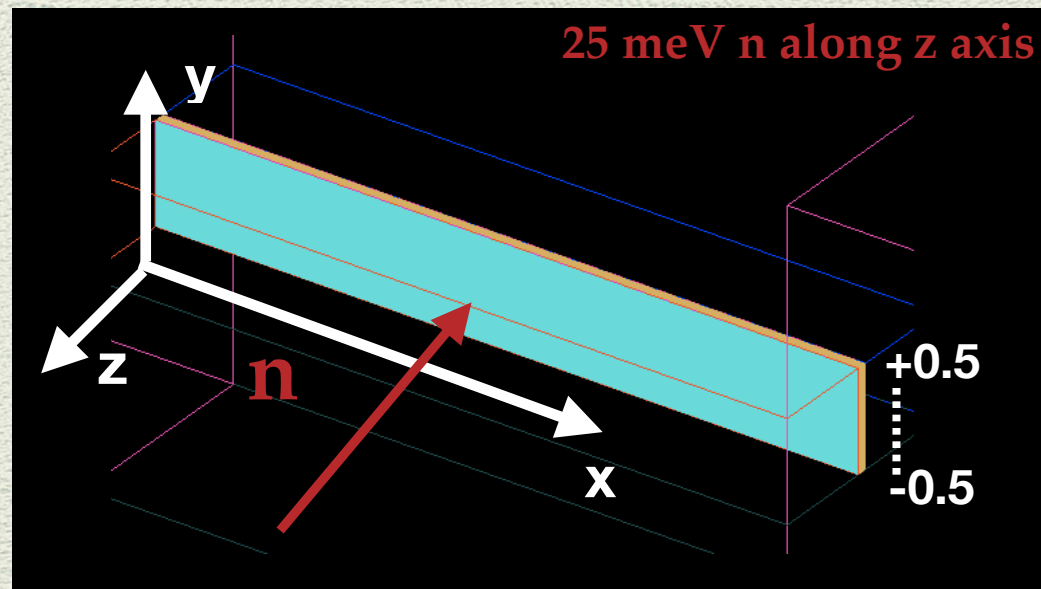
from $y=-0.50\text{cm}$ to $y=-0.40\text{cm}$



- Electron Spatial distribution (elec/cm²/pr) has been derived from the energy deposition density (GeV/cm³/pr) of charged particles dividing by $w=28$ eV and integrating on the y coordinate.
- An energy threshold condition has been set in such a way that the energy deposition has been taken into account only for alphas with kinetic energy greater than 104 eV (ionization potential).
- Finally the spatial binning used for the estimation of the energy deposition spatial bin $\delta y=0.02$ for $y[-0.1;0.1]$

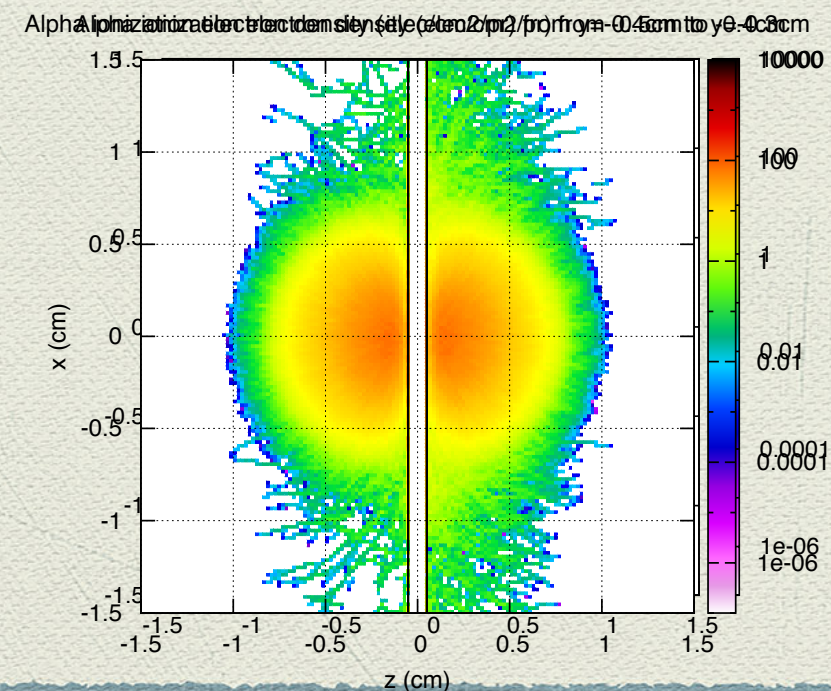


Indirectly derived electron density (transversal xz section)

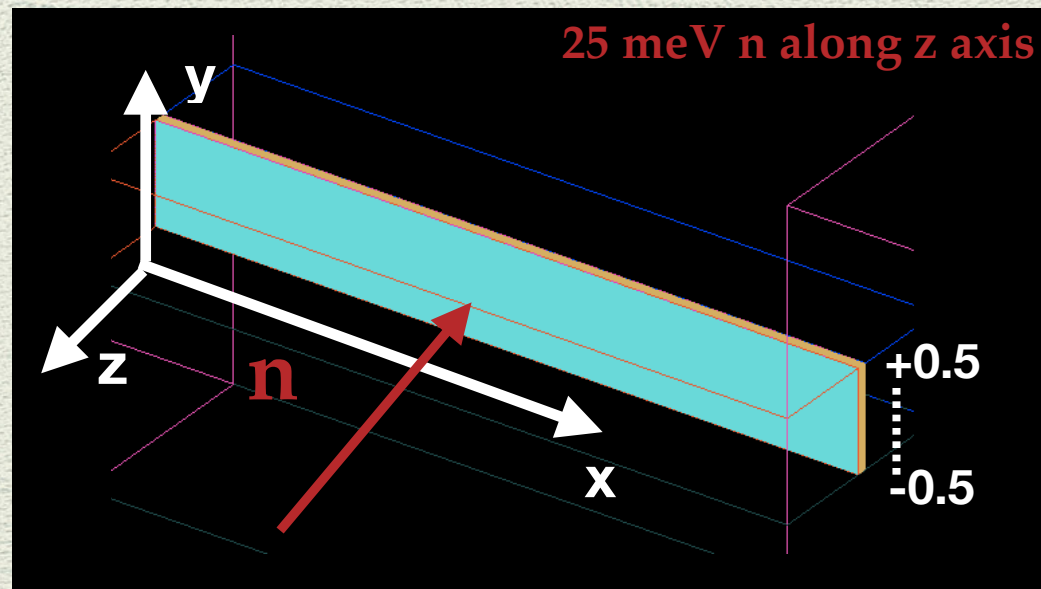


from $y = -0.50\text{cm}$ to $y = -0.40\text{cm}$
 from $y = -0.40\text{cm}$ to $y = -0.30\text{cm}$

- Electron Spatial distribution (elec/cm²/pr) has been derived from the energy deposition density (GeV/cm³/pr) of charged particles dividing by $w = 28\text{ eV}$ and integrating on the y coordinate.
- An energy threshold condition has been set in such a way that the energy deposition has been taken into account only for alphas with kinetic energy greater than 104 eV (ionization potential).
- Finally the spatial binning used for the estimation of the energy deposition spatial bin $\delta y = 0.02$ for $y[-0.1; 0.1]$

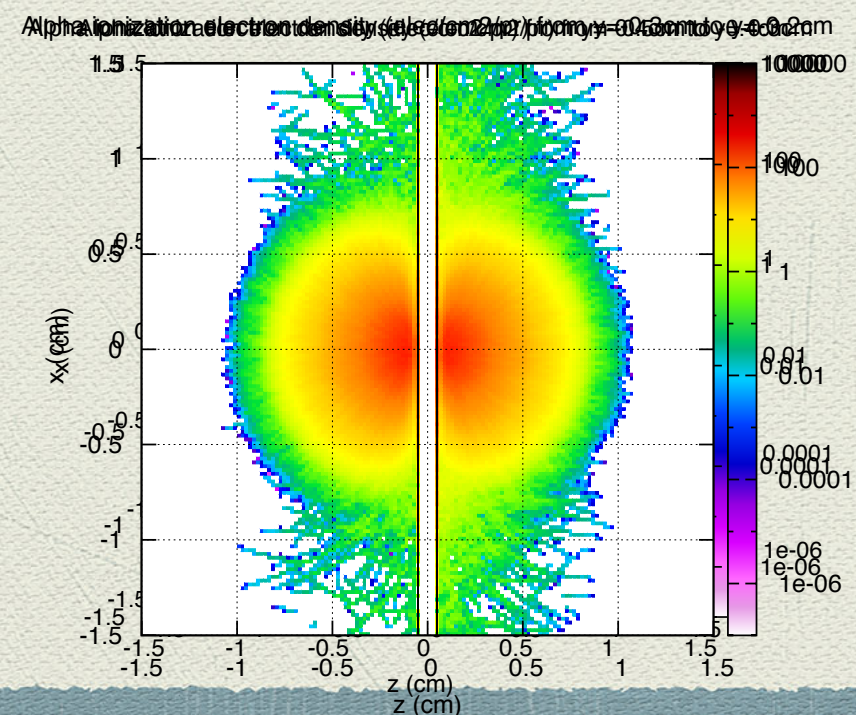


Indirectly derived electron density (transversal xz section)

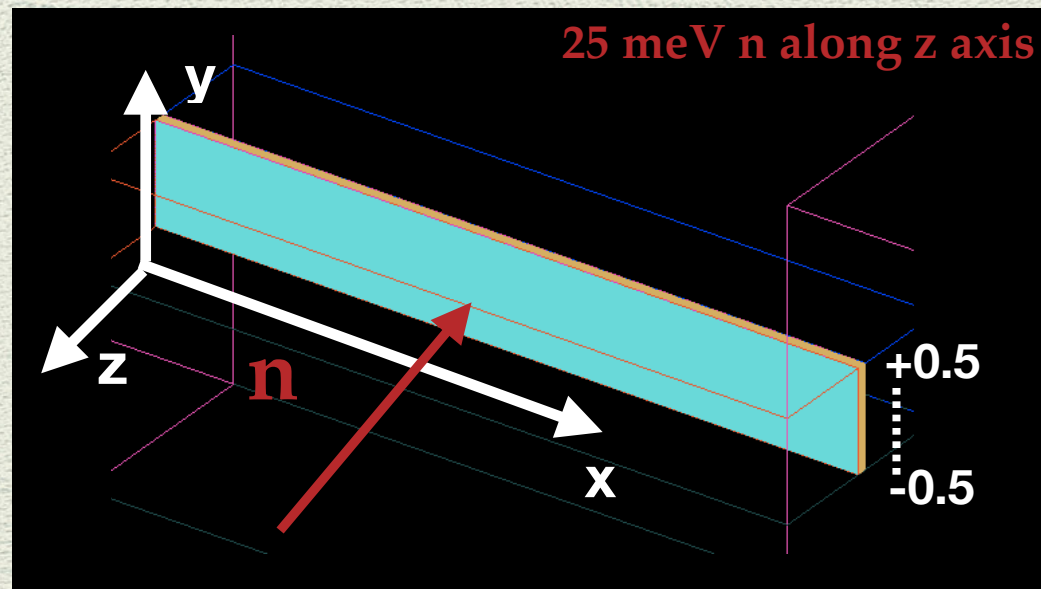


from $y = -0.50\text{cm}$ to $y = -0.40\text{cm}$
 from $y = -0.40\text{cm}$ to $y = -0.30\text{cm}$
 from $y = -0.30\text{cm}$ to $y = -0.20\text{cm}$

- Electron Spatial distribution (elec/cm²/pr) has been derived from the energy deposition density (GeV/cm³/pr) of charged particles dividing by $w = 28\text{ eV}$ and integrating on the y coordinate.
- An energy threshold condition has been set in such a way that the energy deposition has been taken into account only for alphas with kinetic energy greater than 104 eV (ionization potential).
- Finally the spatial binning used for the estimation of the energy deposition spatial bin $\delta y = 0.02$ for $y[-0.1; 0.1]$

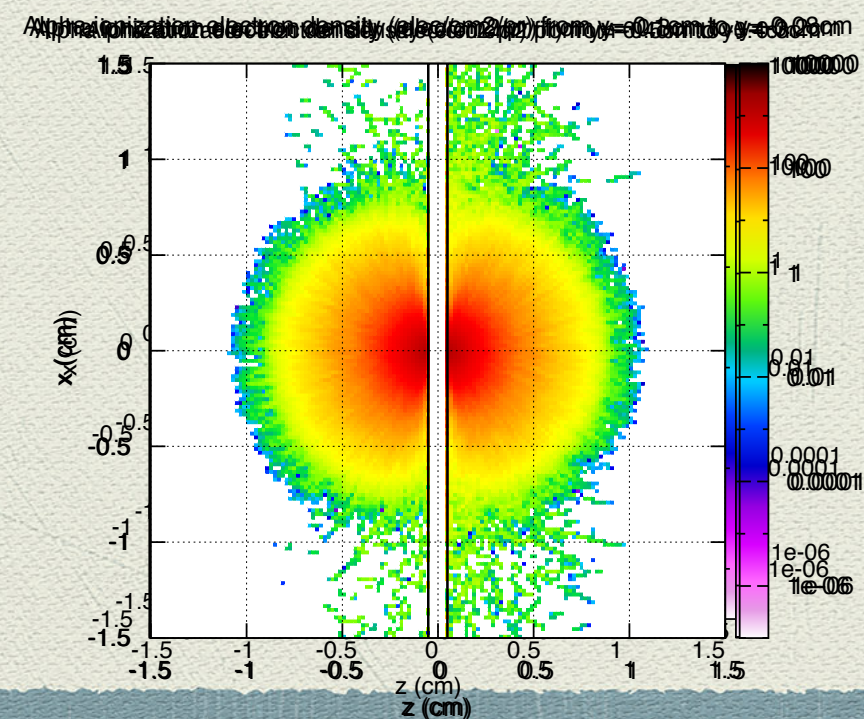


Indirectly derived electron density (transversal xz section)

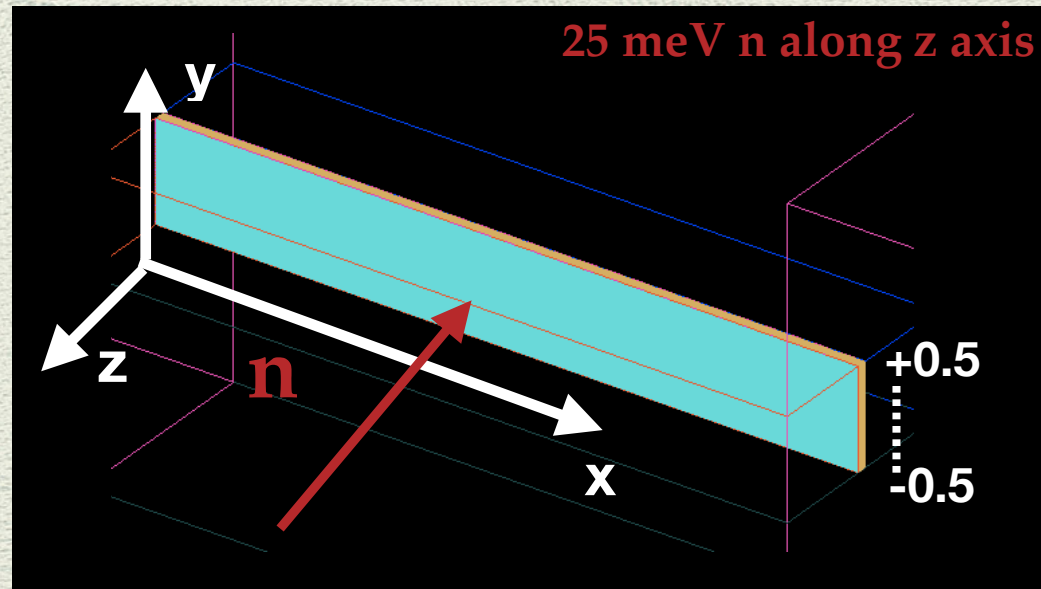


from $y = -0.50\text{cm}$ to $y = -0.40\text{cm}$
 from $y = -0.40\text{cm}$ to $y = -0.30\text{cm}$
 from $y = -0.30\text{cm}$ to $y = -0.20\text{cm}$
 from $y = -0.10\text{cm}$ to $y = -0.08\text{cm}$

- Electron Spatial distribution (elec/cm²/pr) has been derived from the energy deposition density (GeV/cm³/pr) of charged particles dividing by $w = 28\text{ eV}$ and integrating on the y coordinate.
- An energy threshold condition has been set in such a way that the energy deposition has been taken into account only for alphas with kinetic energy greater than 104 eV (ionization potential).
- Finally the spatial binning used for the estimation of the energy deposition spatial bin $\delta y = 0.02$ for $y[-0.1; 0.1]$

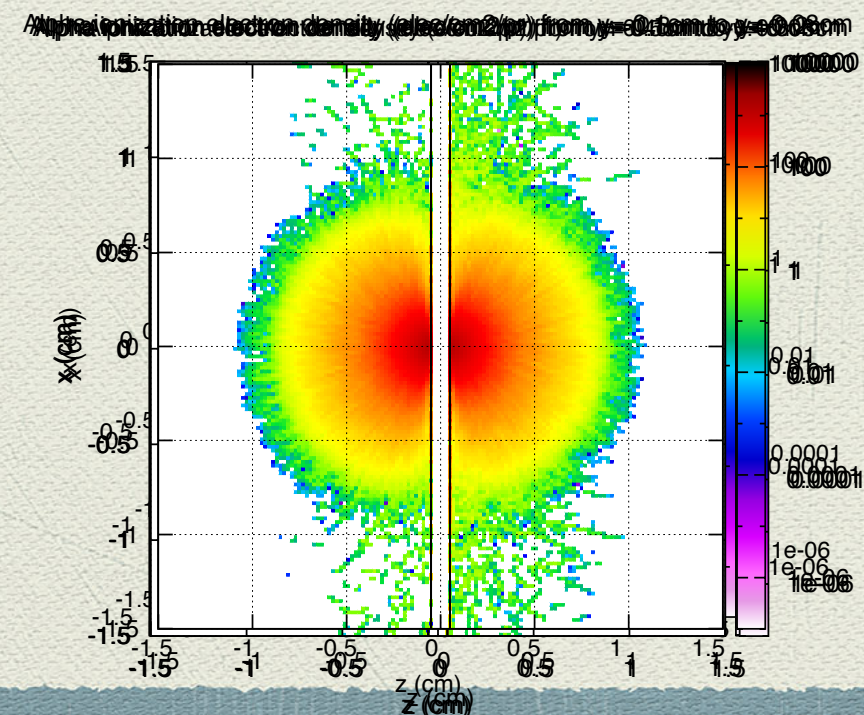


Indirectly derived electron density (transversal xz section)

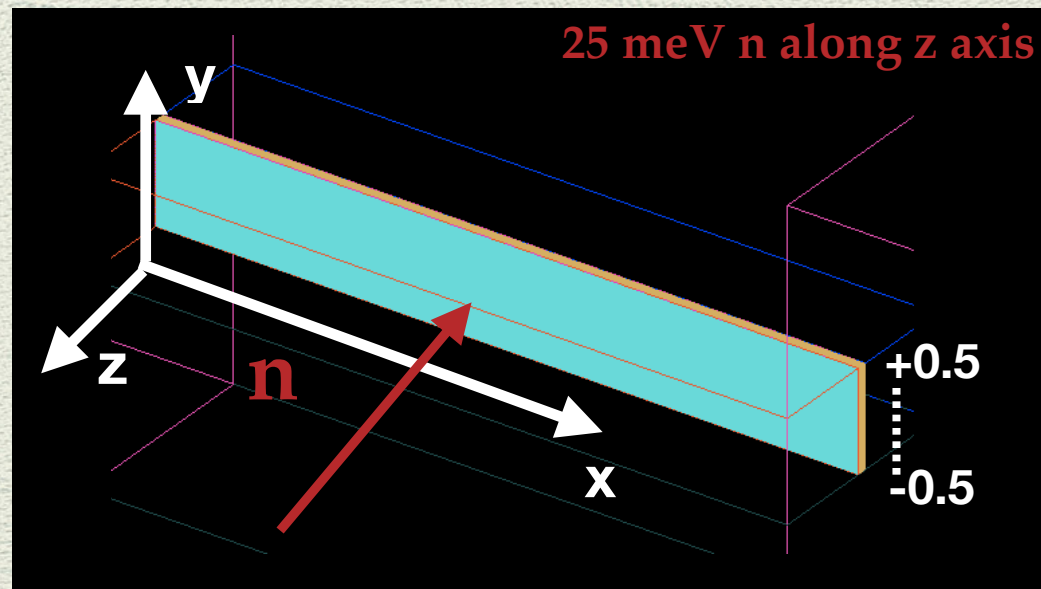


from $y = -0.50\text{cm}$ to $y = -0.40\text{cm}$
 from $y = -0.40\text{cm}$ to $y = -0.30\text{cm}$
 from $y = -0.30\text{cm}$ to $y = -0.20\text{cm}$
 from $y = -0.10\text{cm}$ to $y = -0.08\text{cm}$
 from $y = -0.06\text{cm}$ to $y = -0.04\text{cm}$

- Electron Spatial distribution (elec/cm²/pr) has been derived from the energy deposition density (GeV/cm³/pr) of charged particles dividing by $w = 28\text{ eV}$ and integrating on the y coordinate.
- An energy threshold condition has been set in such a way that the energy deposition has been taken into account only for alphas with kinetic energy greater than 104 eV (ionization potential).
- Finally the spatial binning used for the estimation of the energy deposition spatial bin $\delta y = 0.02$ for $y[-0.1; 0.1]$



Indirectly derived electron density (transversal xz section)



from $y = -0.50\text{cm}$ to $y = -0.40\text{cm}$

from $y = -0.40\text{cm}$ to $y = -0.30\text{cm}$

from $y = -0.30\text{cm}$ to $y = -0.20\text{cm}$

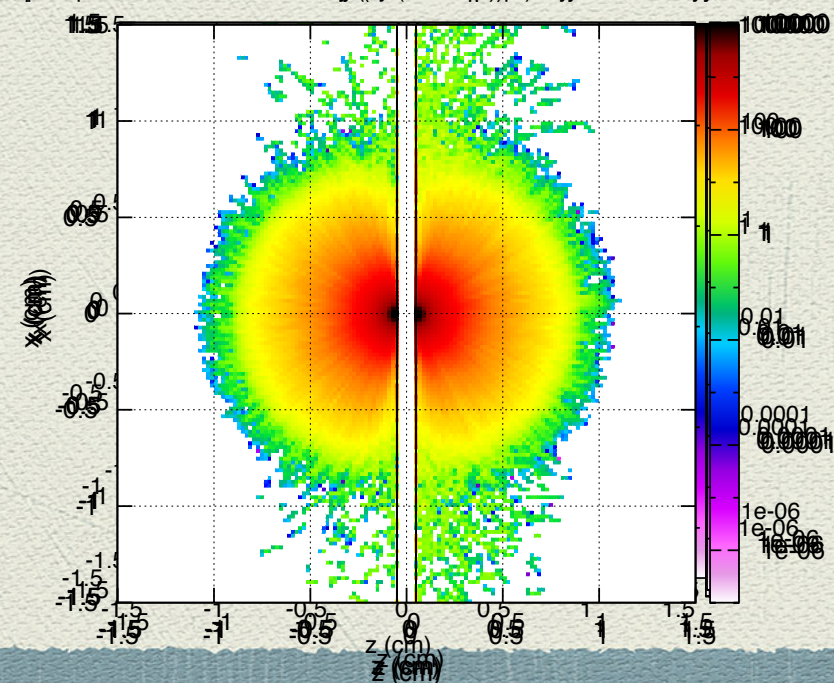
from $y = -0.10\text{cm}$ to $y = -0.08\text{cm}$

from $y = -0.06\text{cm}$ to $y = -0.04\text{cm}$

from $y = -0.02\text{cm}$ to $y = -0.00\text{cm}$

- Electron Spatial distribution (elec/cm²/pr) has been derived from the energy deposition density (GeV/cm³/pr) of charged particles dividing by $w = 28\text{ eV}$ and integrating on the y coordinate.
- An energy threshold condition has been set in such a way that the energy deposition has been taken into account only for alphas with kinetic energy greater than 104 eV (ionization potential).
- Finally the spatial binning used for the estimation of the energy deposition spatial bin $\delta y = 0.02$ for $y[-0.1;0.1]$

Approximative electron density (elec/cm²/pr) from $y = -0.10\text{cm}$ to $y = 0.08\text{cm}$



Multiple sheet detector geometric configuration optimization

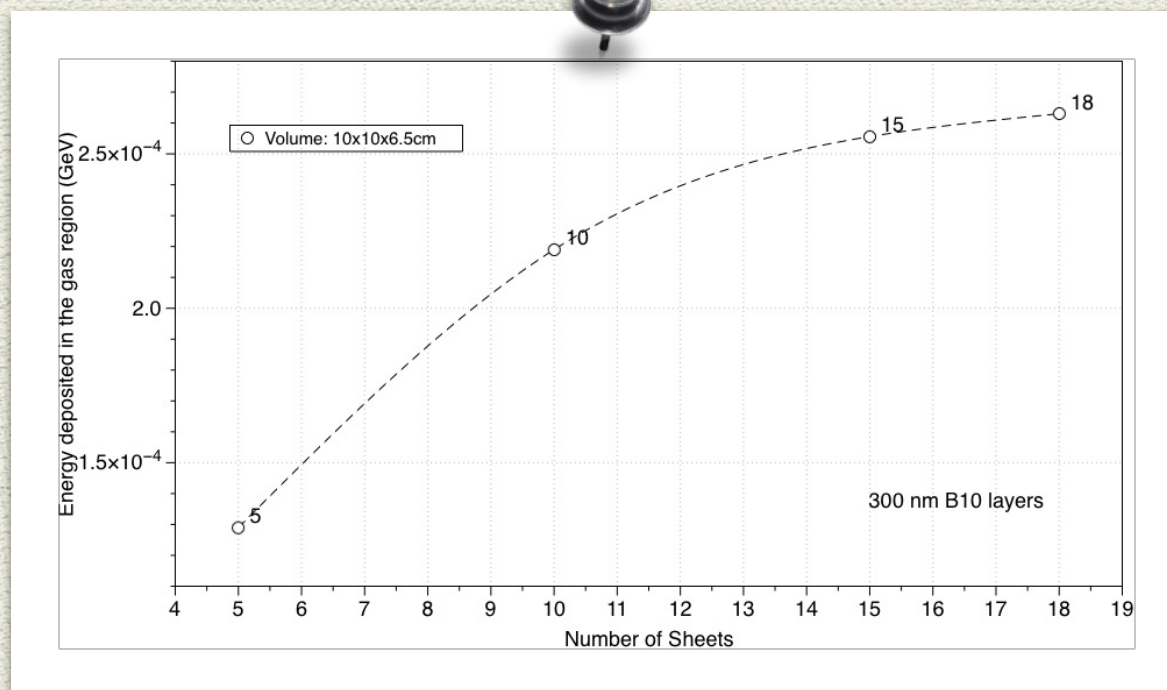
Optimal configuration with respect to maximise the number of charged particles that can ionise the gas region

A. Optimal distance among sheets (fixing the coating thickness and the volume)

Energy deposited by the charged particles in the gas as a function of the number of sheets in a fixed volume with two-side 300nm B-10 thickness

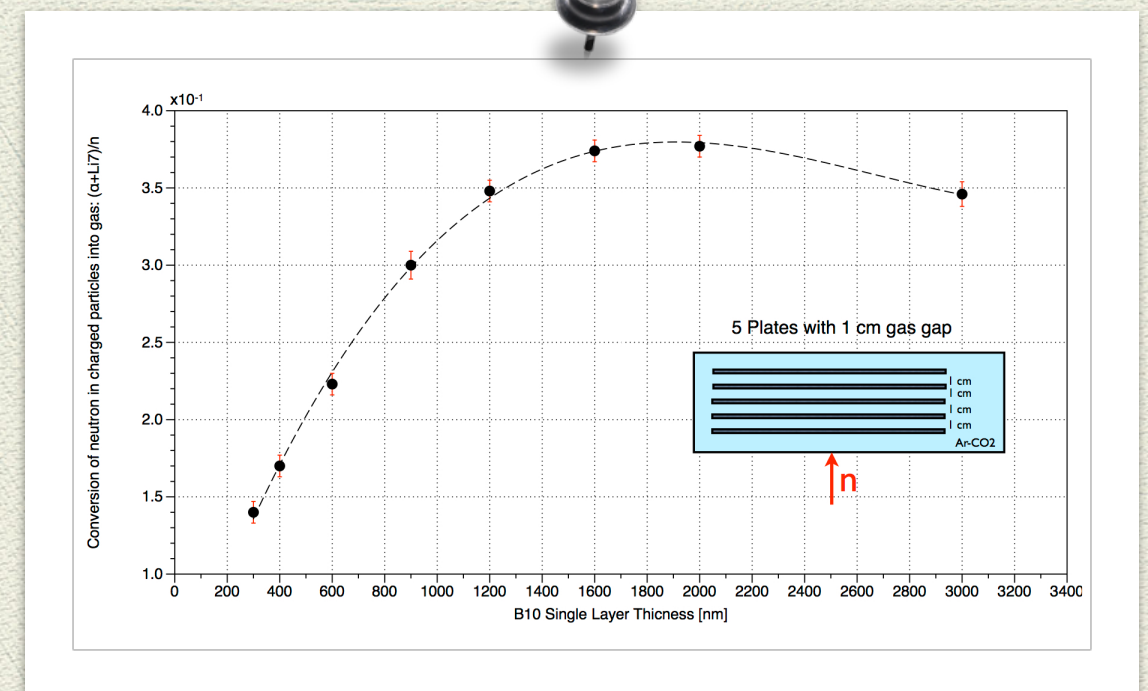
Four cases have been simulated: 5, 10, 15, 18

(gas gap, respectively, 1cm, 0.5 cm, 0.3125cm and 0.25cm)



The total energy deposition in the considered fixed volume is expected to increase of about 70% doubling the number of plates from 5 to 10 (i.e. reducing the gap from 1 to 0.5 cm), but less than 20% going from 10 to 18 (i.e. reducing the gap from 0.5 cm to 0.25 cm).

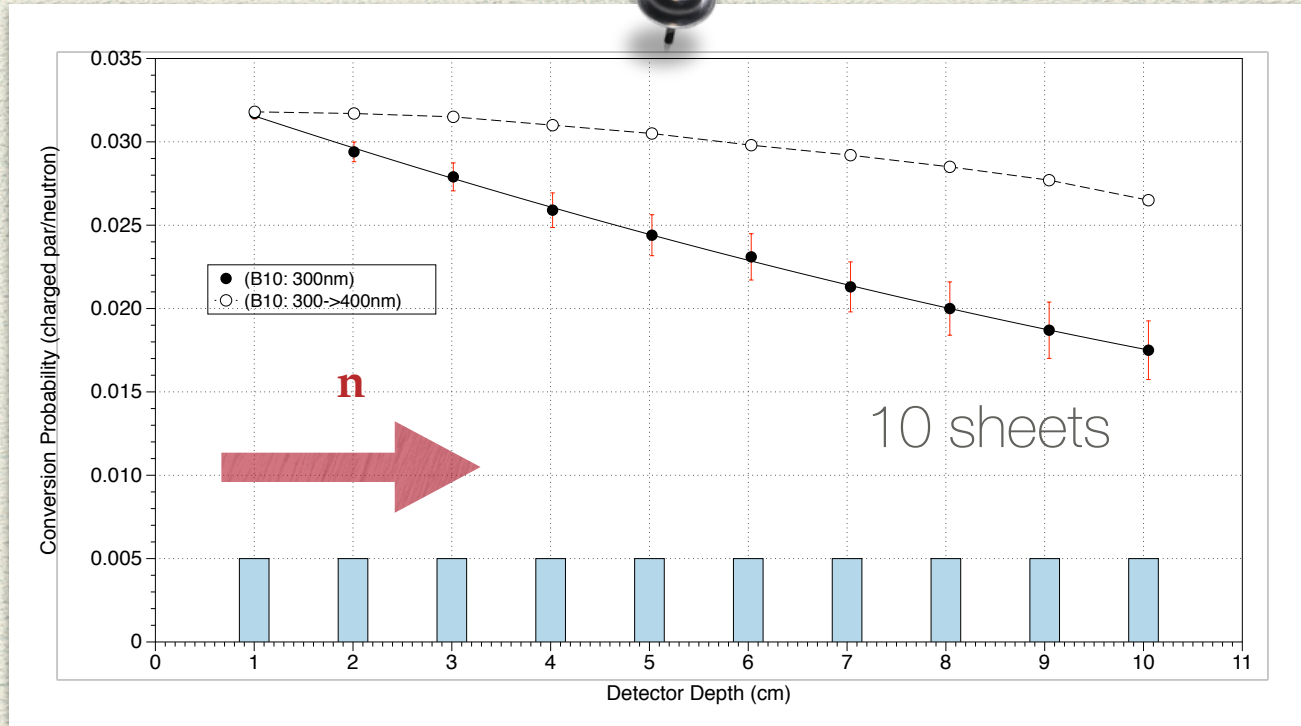
B. Optimal thickness of the coating (fixing the number of sheets and the relative distance)



This analysis shows that an optimum ¹⁰B thickness exists for a given volume and number of sheets: in case of 5 sheets it is around 1900 nm.

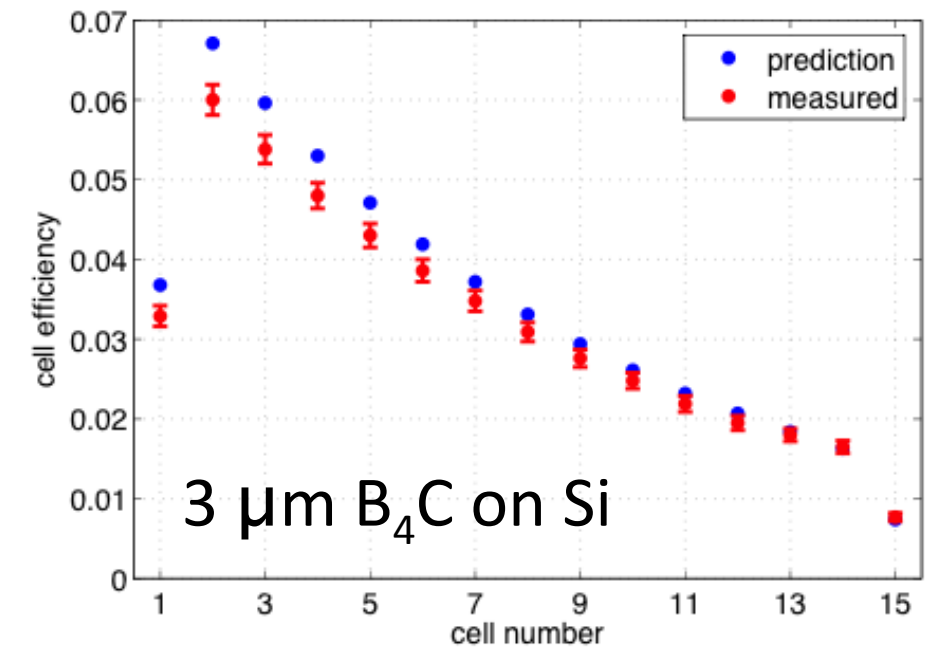
“Shadowing Effect”: envisaging a solution

Measurements and Simulations for thermal neutrons



workshop ILL – 2012-03-13/14

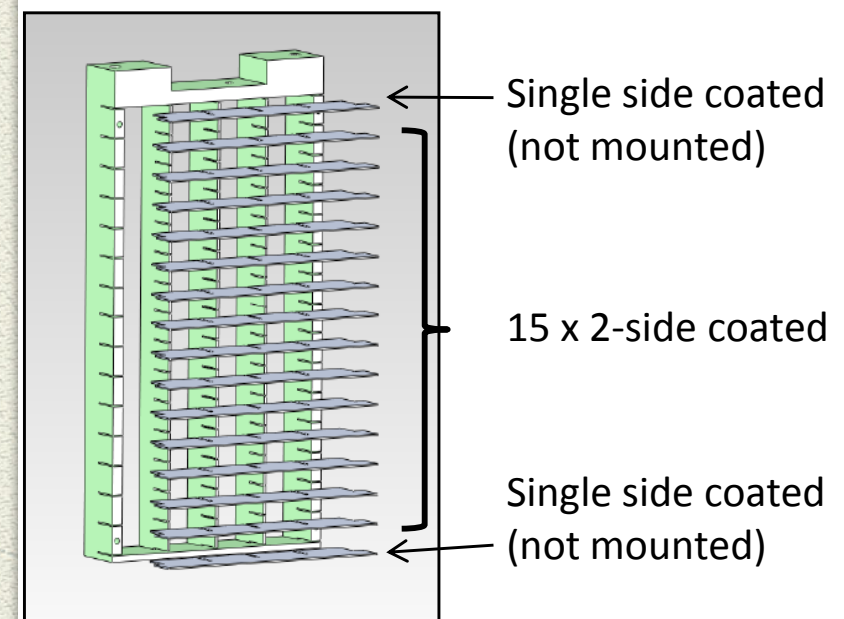
Efficiency per cell



2012-03-13/14 | carina.hoglund@esss.se

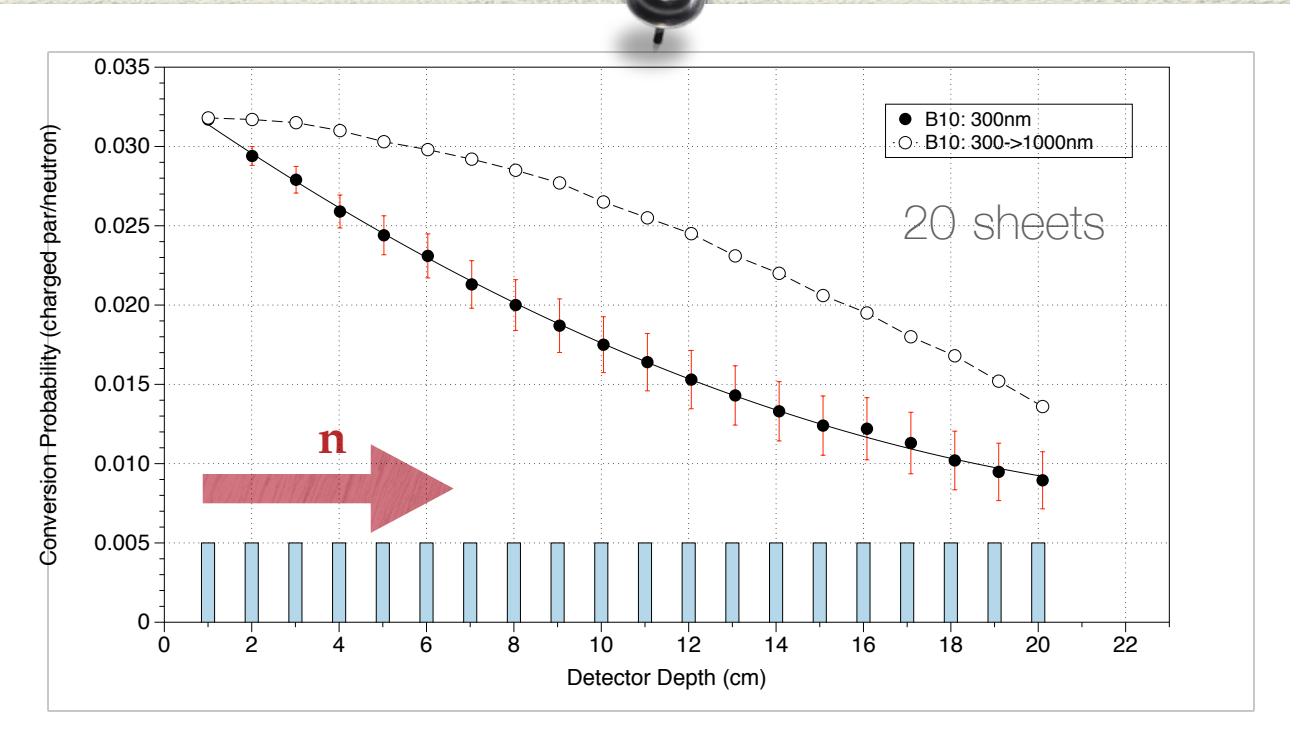
- Estimated conversion efficiency in the case of 10 and 20 sheets detector (1cm apart 300nm B-10 thickness 2-side coated).
- Monochromatic Thermal neutron (25 meV)
- The shadowing effect can be mitigated by using a non-constant ^{10}B coating along the neutron path inside the detector (open dot in the plots)
- This effect has been measured by ESS team (see reference) in a similar detector configuration

Each grid: 17 Al-blades, 20 x 80 x 0.5 mm³

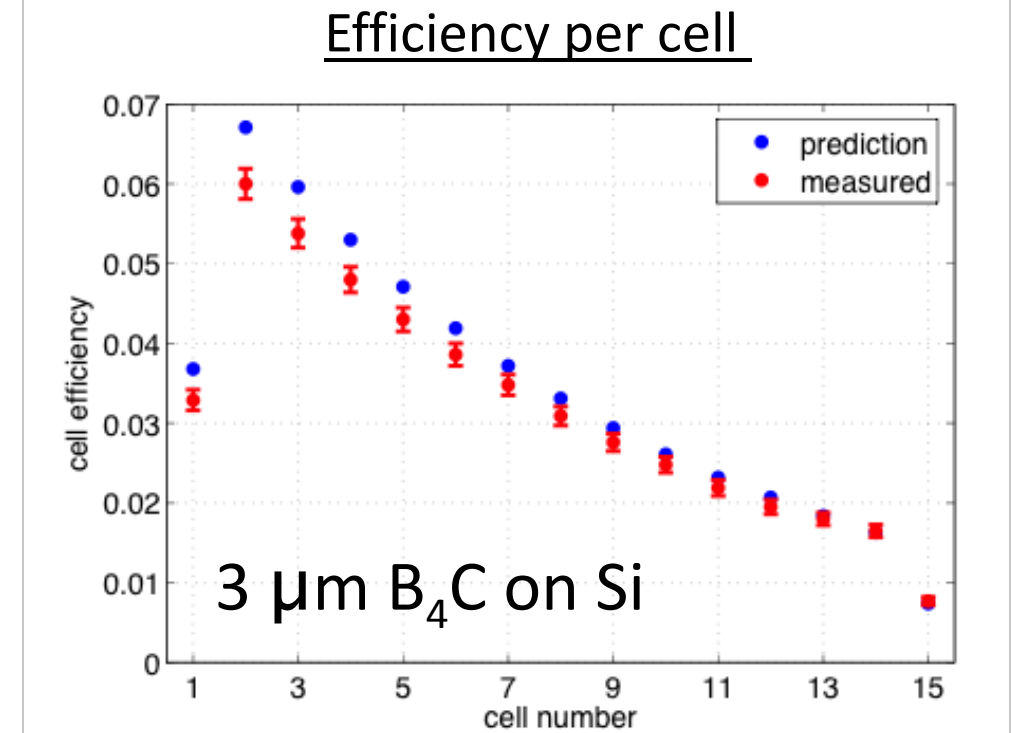


“Shadowing Effect”: envisaging a solution

Measurements and Simulations for thermal neutrons



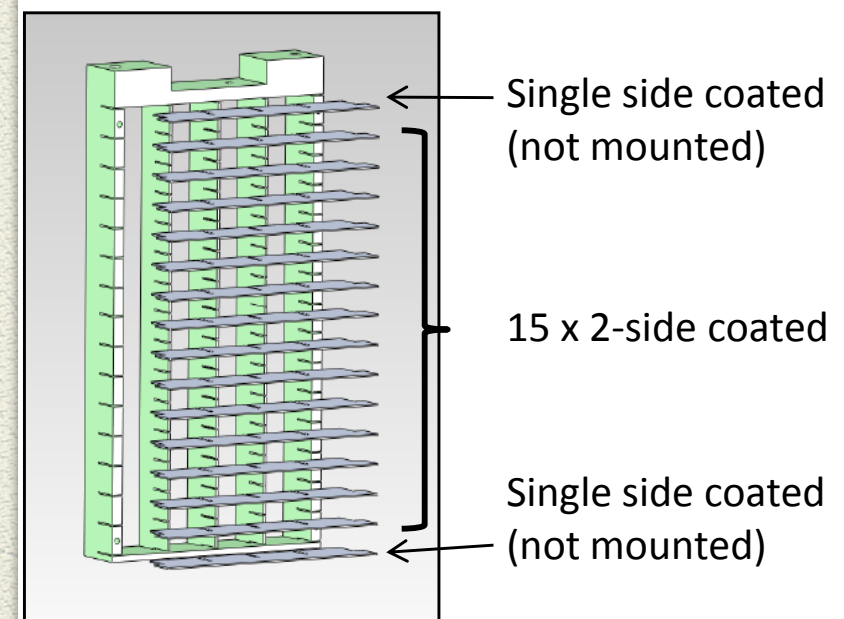
workshop ILL – 2012-03-13/14



2012-03-13/14 | carina.hoglund@esss.se

- Estimated conversion efficiency in the case of 10 and 20 sheets detector (1cm apart 300nm B-10 thickness 2-side coated).
- Monochromatic Thermal neutron (25 meV)
- The shadowing effect can be mitigated by using a non-constant ¹⁰B coating along the neutron path inside the detector (open dot in the plots)
- This effect has been measured by ESS team (see reference) in a similar detector configuration

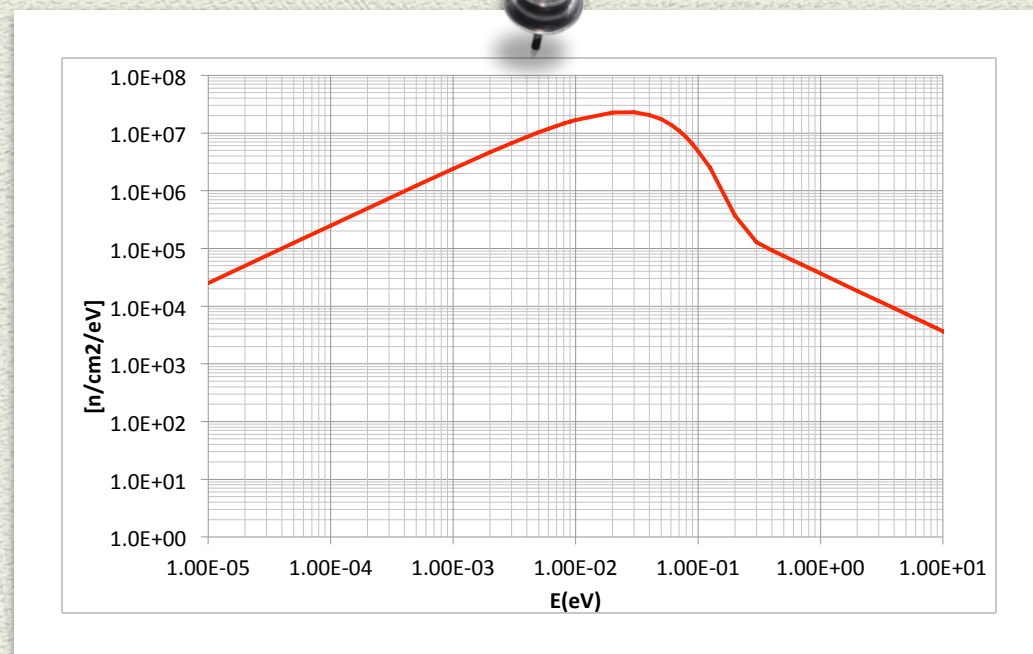
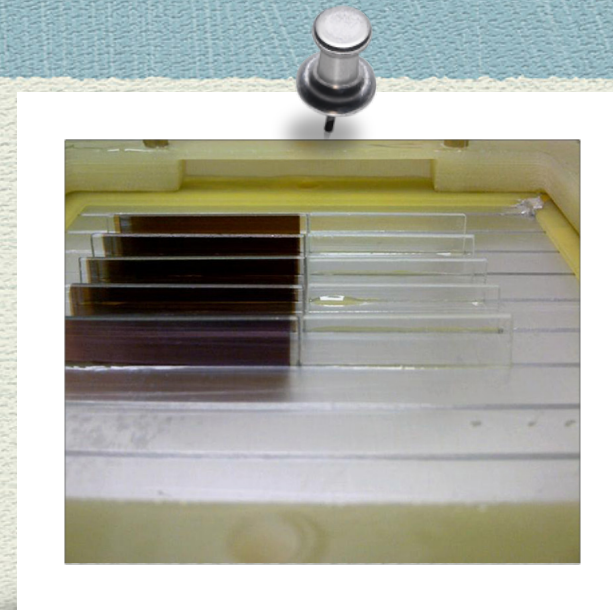
Each grid: 17 Al-blades, 20 x 80 x 0.5 mm³



MC predictions and experimental results: Comparison for 5 sheets detector at ENEA TRIGA

TRIGA reactor at the ENEA-Centro Ricerche Casaccia (Rome):

The reactor can be operated at different powers from a few Watt to 1 MW with a neutron flux of about $2 \cdot 10^6$ n/cm²/s at the maximum power, whose spectrum is shown in the picture



Conv. Efficiency	MC	Exp
ϵ [%]	7.6 ± 0.6	4.3 ± 0.5

Difference between MC prediction and the measurement likely due to:

- (1) the overall charge production/amplification/threshold in the detector stages, that is not included in the MC model;
- (2) a possible contamination of B₂O₃ and the reduced density of the films with respect to the bulk value in the conversion film (importance of the spectrometric analysis of the layer)
- (3) The experimental contribution of the external face of the first sheet is lost, whilst it has been taken into account in the simulation

Conclusion: future plan

- ◆ Simulation with MCNPX/PHITS in order to solve the discrepancies found between Fluka and Geant4
- ◆ Efficiency versus neutron energy, angular incidence and other major parameters
- ◆ Modelling the gas ionisation more accurately (**interfacing with specialised gas detector code as Garfield**)
- ◆ Estimate how could change the efficiency using Li-6 or Gd-155, Gd-157 in spite of B-10
- ◆ PHITS as interesting alternative to FLUKA for the transport of some heavy ion.

In fact in FLUKA, **recoil protons and protons** from $N(n,p)$ reaction are produced and transported explicitly, taking into account the detailed kinematics of elastic scattering, continuous energy loss with energy straggling, delta ray production, multiple and single scattering. The same applies to light fragments (**alpha, 3-H**) from **neutron capture in 6-Li and 10-B**, if pointwise transport has been requested by the user. **All other charged secondaries, including fission fragments, are not transported but their energy is deposited at the point of interaction (kerma approximation).**

Thank you for your attention